Asian Review of Mechanical Engineering
ISSN: 2249-6289 (Print) | 3049-1886 (Online)
Journal Homepage: https://armejournal.org
DOI: https://doi.org/10.70112/arme-2026.15.1.4334

Review Article

Integrated Mist Assisted and Composite Cooling Architectures for Ultra High Temperature Gas Turbines: Advances, Multiphysics Modelling, and Future Directions Beyond 2000 K

Muhammad Haris Malik[1*], Muhammad Faisal[2], Zaryab Basharat[3], Syeda Javeria Sajid[4], Muhammad Faizan Kahloon[5] and Fazal E Wadood[6]
[1,2,5]Department of Fluid Machinery and Engineering, [3]MOE Key Laboratory of Thermo-Fluid Science and Engineering, [4]School of Materials Science and Engineering, Xi'an Technological University, Xi'an, China
[6]School of Engineering and the Environment, Kingston University, London, United Kingdom

Article Information

Article History
Received:
Revised:
Accepted:
Published online:

Keywords
Mist-Assisted Cooling
Gas Turbine Thermal Management
Two-Phase Heat Transfer
Thermal Barrier Coatings
Additive Manufacturing for Cooling Structures

Correspondence
muhammadharismalik3@gmail.com

ORCID
Muhammad Haris Malik
https://orcid.org/0009-0008-1618-4699
Muhammad Faisal
https://orcid.org/0009-0007-4415-2558
Zaryab Basharat
https://orcid.org/0009-0008-1914-3331
Syeda Javeria Sajid
https://orcid.org/0009-0001-2385-7707
Muhammad Faizan Kahloon
https://orcid.org/0009-0009-4011-6669
Fazal E Wadood
https://orcid.org/0000-0003-4752-4357

Abstract

Efficient thermal management is critical to enabling gas turbine operation at increasingly higher inlet temperatures. This review critically examines the integration of mist-assisted cooling with established impingement and film-cooling methods and positions it alongside six emerging innovation pillars: composite cooling architectures, additively manufactured lattice and truss structures, two-phase working fluids (steam/mist and heat pipes), advanced thermal barrier coatings, and surface-modification techniques (dimples and vortex generators). Through a systematic analysis of more than 150 experimental and numerical studies, we identify the dominant variables-droplet loading, size distribution, nozzle geometry, Reynolds number, heat flux, and surface curvature-that govern mist-enhanced heat-transfer performance. We further explore how mist cooling synergizes with passive insulation strategies to extend effective coverage and uniformity under realistic turbine geometries and operating conditions. Finally, we evaluate cutting-edge diagnostic and simulation tools, highlight critical knowledge gaps in droplet dynamics and corrosion resistance, and propose targeted research directions for developing robust, multifunctional cooling solutions capable of sustaining turbine inlet temperatures beyond 2000 K.

I. INTRODUCTION

The relentless pursuit of enhanced thermodynamic efficiency and specific power output in modern gas turbine engines, critical for applications ranging from power generation to aviation propulsion, necessitates operation at ever-increasing turbine inlet temperatures (TITs). These temperatures now routinely exceed the melting points of the high-performance nickel-based superalloys used in the first-stage turbine blades and vanes-the most thermally stressed components within the

engine. Consequently, sophisticated cooling strategies have become not merely beneficial but essential for ensuring the structural integrity, durability, and extended operational life catastrophic creep deformation or melting, thereby supporting engine reliability and availability. The evolution of gas turbine blade cooling reflects a continuous engineering effort to manage escalating thermal loads. Initial reliance on simple convection cooling within smooth internal passages rapidly proved inadequate. This led to the development and maturation of techniques such as turbulator-enhanced internal convection (ribs and pins), impingement cooling for leading edges, and film cooling, wherein relatively cool air extracted from the compressor is injected through discrete holes to establish an insulating protective layer on the external surface of the blade. Each generation introduced greater complexity and integration, pushing the boundaries of manufacturing capabilities and heat-transfer understanding. Gas turbines play a vital role in numerous applications, including aviation systems [1], electricity generation [2], and propulsion technologies [3]. Improving the efficiency of these systems is closely linked to lowering emissions in both the aviation and power generation sectors. Consequently, significant research attention has been given to developing advanced technologies that enhance the performance of gas turbines and their associated systems. Modern improvements include increasing turbine inlet temperatures, developing advanced blade materials, implementing more effective cooling methods, applying thermal barrier coatings, optimizing blade aerodynamic design, and minimizing various system losses. Among these approaches, operating at higher turbine inlet temperatures is widely recognized as one of the most effective methods for improving performance. Contemporary gas turbine engines typically operate at elevated temperatures ranging from approximately 1100 °C to 1600 °C, which increases power output and improves thermal efficiency [4].

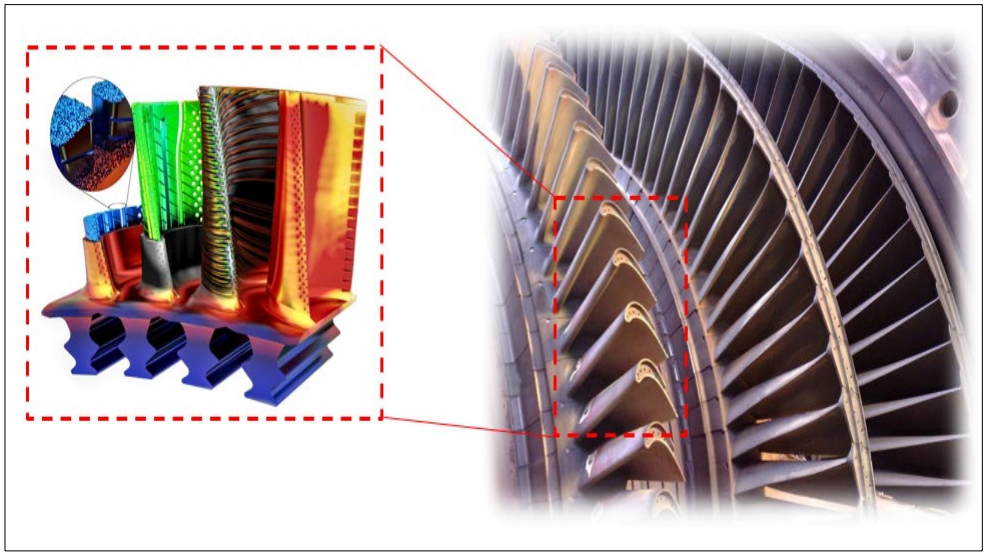

Fig.1 Gas Turbine Blade Cooling Structure

However, higher operating temperatures also intensify heat transfer to turbine blades. The resulting temperature gradients within the blade material can generate thermal stresses, which must be controlled to preserve structural integrity. Because the temperature of turbine blades can exceed the allowable limits of the metallic materials, efficient cooling techniques are essential. In most cases, cooling is achieved by diverting a portion of compressed air from the engine compressor to the turbine blades.

Reducing the amount of compressor bleed air used for cooling is beneficial for overall engine efficiency, since it allows more air to participate in the main combustion process at higher temperatures. Nevertheless, extracting this cooling air introduces a performance penalty that affects the overall thermal efficiency of the system. Therefore, a thorough understanding of turbine blade cooling mechanisms and operating conditions is crucial for achieving reliable and efficient gas turbine performance.

This research begins with a brief introduction to two critical turbine cooling techniques: mist impingement cooling and thermal barrier coatings (TBC). First, the principles and applications of mist impingement cooling are explored, followed by an in-depth examination of thermal barrier coatings and their role in enhancing turbine performance. A comprehensive review of these two techniques is provided, highlighting their effectiveness in improving cooling performance and prolonging the service life of turbine components. Subsequently, the report delves into recent advancements in turbine cooling, focusing on modern techniques that range from cutting-edge numerical simulations to the incorporation of real-time thermal monitoring systems. Additionally, the utilization of alternative cooling liquids and other innovative methods is

discussed, reflecting the ongoing evolution in turbine cooling technologies.

A. Fundamentals of Gas Turbine Blade Heat Transfer

The thermal management of first-stage turbine blades represents one of the key challenges associated with gas turbine design, driven by combustion gas temperatures (1700–2000 °C) that exceed the melting point (1200–1350 °C) of nickel-based superalloy substrates [5]. These extreme gas-path conditions generate heat fluxes surpassing 2 MW/m² at the blade leading edge due to forced convection from high-velocity combustion gases ($h_g \approx 1000–3000$ W/m²·K) [6]. The stagnation region experiences peak thermal loading, while the pressure and suction surfaces exhibit spatially varying heat-transfer coefficients due to boundary-layer acceleration and separation effects. Radiation from particulate-laden combustion products contributes 10–30% of the total incident heat flux at ultra-high temperatures, becoming increasingly significant above 1500 °C [7].

TABLE I REGIONAL VARIATION OF HEAT TRANSFER MECHANISMS IN TURBINE BLADES

Blade Region	Primary Heat Input Mechanism	Key Heat Rejection Mechanism	Radiation Contribution
Leading Edge	Forced Convection (Stagnation)	Impingement Jet Cooling	15-30% [9]
Pressure Surface	Forced Convection (Accelerating)	Rib/Pin-finned Channels	10-20% [10]
Suction Surface	Forced Convection (High Speed)	Smooth/Pedestal Channels	5-15% [10]
Trailing Edge	Forced Convection + Wake Effects	Pin Banks / Cutback Cooling	<10% [11]

Conjugate heat transfer mechanisms govern thermal energy flow through turbine blades. The primary energy input occurs via external forced convection from hot gases to the blade surface, while conduction transports heat radially through the multilayer wall structure (substrate, bond coat, and TBC). Critical heat rejection occurs through internal convection to coolant fluids within blade passages.

Radiation exchange between the blade surface and the combustion environment supplements heat input, particularly at the leading edges [8]. These mechanisms operate simultaneously in a tightly coupled manner: heat absorbed externally is conducted through the wall and rejected internally via coolant convection. The relative dominance of each mechanism varies significantly by blade region, as quantified in Table I. Effective cooling design must reconcile intense thermal loads with stringent cooling requirements and constraints. The primary objectives are maintaining metal temperatures below creep limits (<850 °C for superalloys) while minimizing thermal gradients to reduce fatigue stresses [12]. These goals are constrained by:

1. Only 15–25% of compressor discharge air is allocated for turbine cooling, creating competition between internal cooling, film cooling, and secondary air systems.
2. Internal cooling effectiveness scales with the pressure ratio (P_c/P_g) between the coolant supply and gas path. Typical design values of 1.05–1.25 limit the maximum achievable heat-transfer coefficients.
3. Bleed air from compressor stages (600–800 °C in modern engines) exhibits reduced heat-absorption capacity compared to ambient coolants.
4. Film-cooling injection can reduce stage efficiency by 2–5% due to boundary-layer disruption and mixing losses.
5. Minimum feature sizes (film holes >0.3 mm, wall thicknesses >0.5 mm) and material durability requirements constrain cooling-design geometry [13].

The complex interplay between these heat-transfer fundamentals and system constraints defines the engineering challenge addressed by advanced cooling technologies.

II. MODERN TURBINE BLADE COOLING TECHNOLOGIES AND EMERGING TRENDS

Gas-turbine power plants will continue to play a pivotal role in the push toward carbon neutrality, driving ever-higher turbine inlet temperatures and demanding novel cooling solutions. Recent progress spans advanced high-temperature materials and coatings, additive-manufactured cooling architectures, effusion and compound cooling methods, and emerging evaporative- and heat-pipe-based approaches. Table II summarizes each trend's core idea, benefits, technical challenges, and key literature.

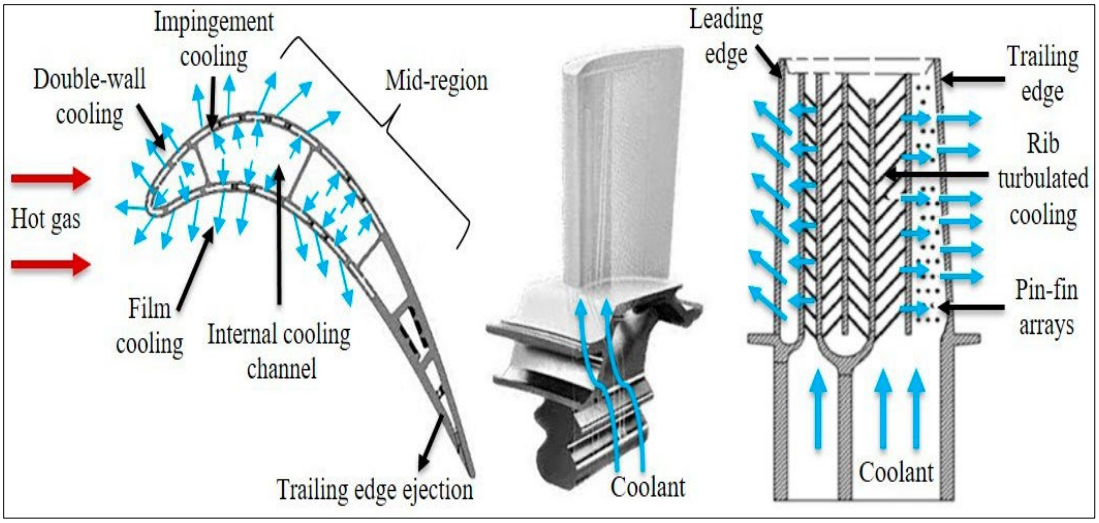

Fig.2 Schematic Representation of Cooling Methods in Gas Turbines [22]

TABLE II RECENT ADVANCES AND TRENDS IN TURBINE-BLADE COOLING TECHNOLOGIES

Trend	Core Concept	Benefits	Challenges	References
High-Temperature Materials & Coatings	Development of nickel- and cobalt-based superalloys, ceramic-matrix composites (CMCs), and advanced thermal barrier coatings (TBCs) with low conductivity and strong adhesion.	Enables operation at >2000 K; extends component life; reduces cooling-air demand.	Thermal mismatch stresses; TBC longevity and spallation; material cost.	[14]
Additive Manufacturing (AM)	Use of powder-bed fusion and other AM methods to fabricate intricate cooling channels, lattices, and film-hole geometries unachievable by casting.	Customizable cooling layouts; minimal pressure drop; high heat-transfer area; rapid design iteration.	Surface finish control; certification and inspection; build defects.	[15,16]
Effusion & Transpiration Cooling	Arrays of micro-holes (effusion) or porous walls (transpiration) to inject coolant uniformly, forming a continuous protective film.	Superior coverage; low jet momentum; uniform surface temperatures.	Micro-fabrication complexity; clogging risk; model validation.	[17]
Compound Cooling Methods	Integration of two or more techniques-e.g., impingement + effusion, jet + swirl, ribs + grooves-to exploit synergistic heat-transfer mechanisms.	Enhanced local heat flux removal; tailored performance; potential to reduce cooling-air usage.	Complex flow interactions; multi-parameter optimization; manufacturing.	[18]
Evaporative (Mist/Spray) Cooling	Introduction of fine water or mist droplets into coolant flow to leverage latent-heat removal and film stability.	Dramatic surface-temperature reductions (100s K); lower coolant mass flow; passive phase-change effects.	Droplet size control; erosion/corrosion; two-phase flow modeling.	[19]
Heat-Pipe Integration	Embedding high-temperature heat pipes (standard, siphon, rotating) within blades or disks to shuttle heat away via phase change and capillary return.	Extremely high effective conductivity; near-isothermal operation; potential to reduce coolant requirements.	Structural integration; fluid return reliability; lifecycle testing.	[20]

A. External Cooling Technology

Film cooling remains the cornerstone of external thermal protection for turbine blades. When coolant is injected through small holes on the blade surface, it creates a thin protective layer that shields against hot-gas impingement. Early efforts focused on cylindrical holes, but challenges in controlling jet–mainstream interactions led to the development of shaped geometries. Fan-shaped holes with compound angles, for example, achieve peak effectiveness at a 30° compound angle on convex walls, minimizing cooling instability [23]. Expanded-hole designs that adjust injection angle, metering length, and expansion angles have demonstrated up to a 32% increase in area-averaged cooling effectiveness using LES compared to RANS predictions [24]. Subsequent innovations explored Y-shaped and converging-slot configurations. Y-holes exhibit superior film coverage, lower local heat-transfer coefficients, and higher adiabatic effectiveness across Reynolds numbers of 50,000–100,000 and blowing ratios of 0.5–2.0 [10]. The round-to-slot hole (RTSH) refines this concept: a circular inlet tapers to a narrow-slit exit, and multi-objective optimization of discharge coefficient and averaged effectiveness further improves performance [25]. Comparative tests confirm that converging-slot designs outperform cylindrical holes in uniformity and coverage [26], [27].

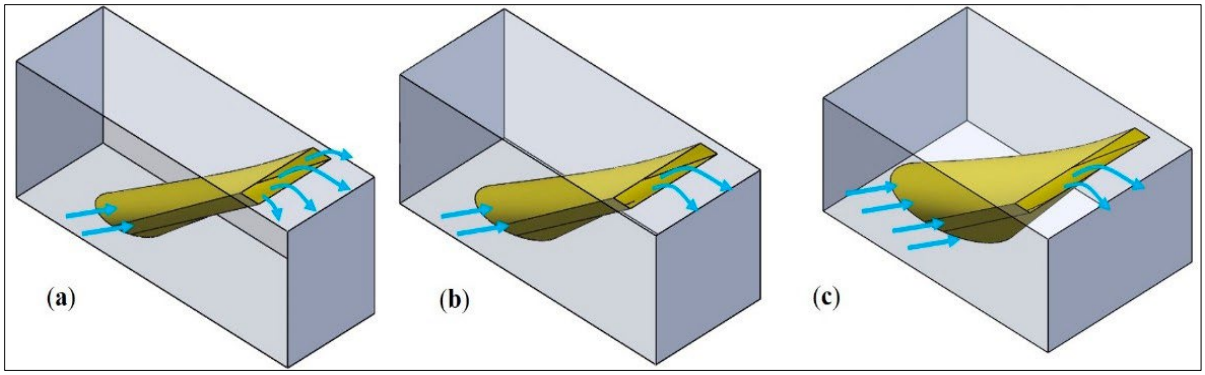

Fig.3 Schematic Illustration of a Typical RTSH Model, Including: (a) The Expansion Hole (b) The Reference Hole [27]

Transpiration cooling merges film-cooling principles with porous-media advantages to deliver uniform, high-coverage thermal protection. Coolant seeps through a porous wall, leveraging its large internal volume and specific surface area to form a continuous, replenishable barrier film (Fig.3). This separation of cooling and load-bearing functions not only enhances heat-exchange efficiency but also allows the protective layer to absorb mechanical impacts independently of the blade's structural components. As a result, transpiration cooling has emerged as one of the most promising external-cooling approaches for next-generation gas turbines and is likely to remain a key research focus given its demonstrated superior performance.

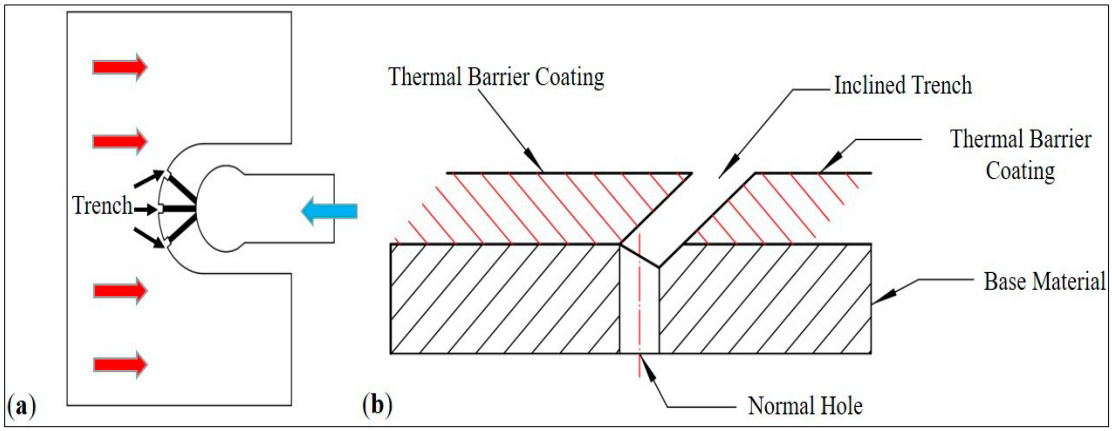

Fig.4 Diagram Showing Typical Trenched Film Holes: (a) Leading-Edge Section, (b) Inclined Trenched Configuration [26]

B. Internal Cooling Technology

Internal cooling methods play a critical role in managing the extreme thermal loads within turbine blades, particularly at hotspots such as the leading edge. Among these methods, jet-impingement cooling stands out as a highly effective technique for enhancing local convective heat transfer. By directing high-speed jets of coolant air onto targeted surfaces, it generates intense localized cooling.

TABLE III COMPARISON OF COOLING TECHNOLOGIES

Category	Technique	Description	Representative Refs.
External	Film Cooling	Discrete, slot, or effusion holes inject coolant to form a surface film; performance depends on hole shape, angle, and arrangement.	[17–24]
	Slot Cooling	Continuous slots replace discrete holes to provide more uniform coverage and are often used in combustor liners.	[24, 25]
Internal	Jet Impingement	High-velocity jets are directed onto blade walls (especially the leading edge) to maximize local heat transfer; performance is sensitive to jet spacing and angle.	[28]
	Rib Turbulators	Periodic ribs in serpentine passages generate vortices and increase wall turbulence; geometry and rotation influence heat-transfer gains.	[29-30]
	Pin-Fin Arrays	Pin fins arranged in channels (typically near the trailing edge) create wake vortices, boosting area-averaged convective coefficients.	[31]

This approach is commonly implemented by configuring internal blade passages to form impingement arrays through strategically placed jets. Several factors influence cooling performance, including jet angle, hole shape and

arrangement, surface roughness, and jet-to-target spacing. Xing *et al.* [32] used the Baseline turbulence model to numerically study the effects of target surface curvature and jet spacing under various crossflow Reynolds numbers (15,000–60,000).

Results showed that curved surfaces enhance heat transfer, and greater jet spacing promotes better jet development. Zhou *et al.* [33] examined the role of jet diameter in single-row impingement arrays and found that although overall flow losses and average heat transfer remained largely unaffected, variations in jet diameter significantly influenced the local mass velocity ratio and heat-transfer uniformity. Xu *et al.* [34] focused on swirling impinging jets (SIJ) emanating from 45° threaded holes and found that jet inclination and spacing had a more pronounced effect on vortex structure than Reynolds number.

Ravanji *et al.* [35] explored jet impingement combined with elliptical pin fins and demonstrated that fins with greater curvature can substantially improve heat-transfer performance. Representative configurations of these internal cooling strategies are shown in Figure7.

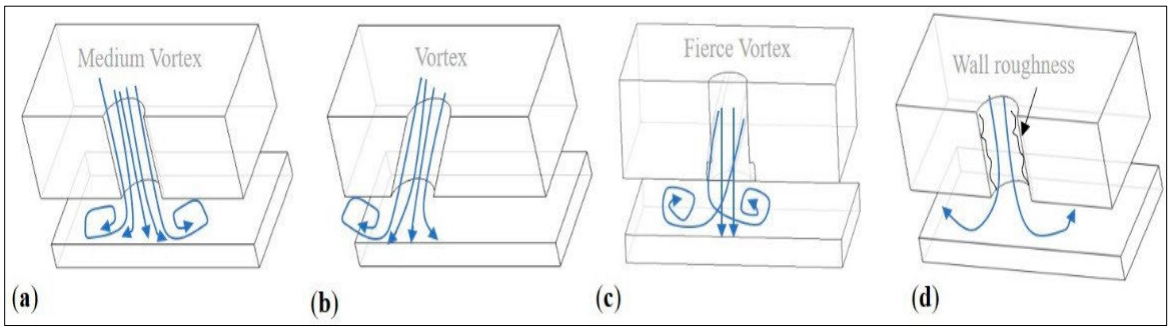

Fig.5 Illustration of the Typical Impingement Cooling Mechanism (a) The Cylinder Hole; (b) The Inclined Hole; (c) The Swirling Hole; (d) The AM Hole [35]

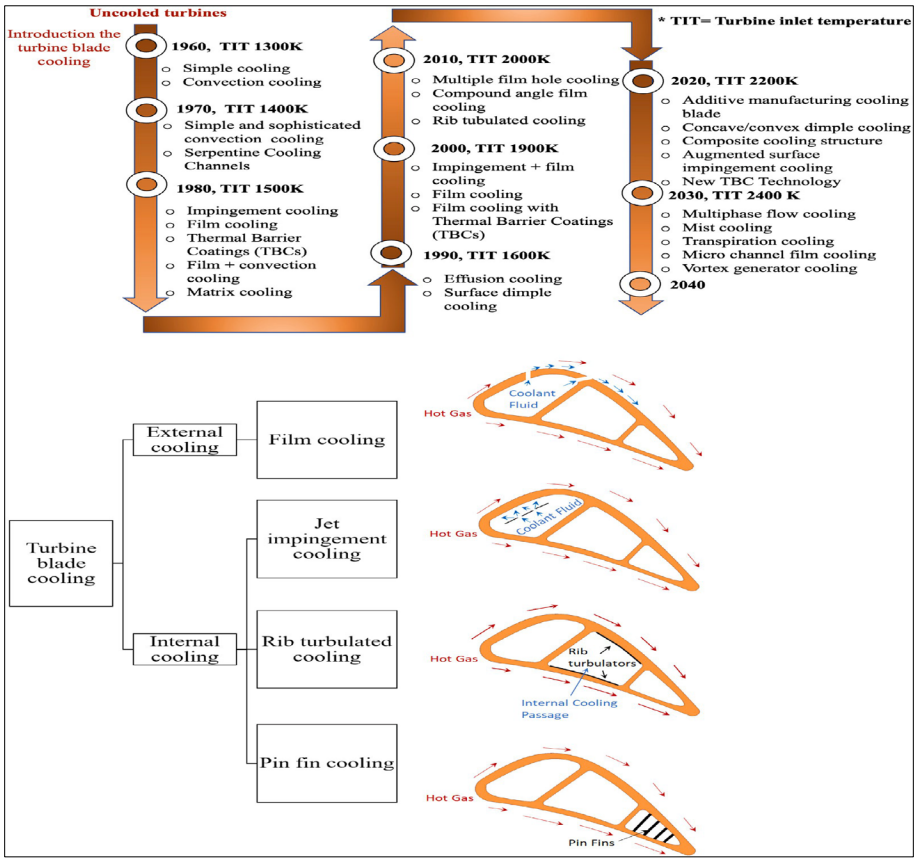

Fig.6 Top: Historical Progression of Turbine Inlet Temperatures Alongside Advancements in Turbine Blade Cooling Technologies Over the Last Seven Decades. Bottom: Major Turbine Blade Cooling Approaches, Classified into Internal and External Cooling Methods, Highlighting the Most Extensively Researched Techniques. [33]

To improve internal cooling performance, turbulence can be enhanced by incorporating ribs, pin fins, truss lattices, or by modifying surface roughness. These methods increase convective heat transfer by disturbing the flow and enlarging the heat-exchange surface.

C. Ribbed Channels

In turbine blade mid-chord regions, where space constraints limit the use of jet impingement, ribbed channels offer a practical solution. Single- and U-shaped channels commonly use various rib geometries-such as inclined, V-shaped, W-shaped, and fin ribs-to enhance heat transfer. Tanda *et al*. [36] studied a high-aspect-ratio channel with 45° ribs and found that adding one longitudinal rib improved thermal performance, but adding two did not offer further benefits. Zhao *et al.* [37] observed that low-profile micro-ribs enhance thermal efficiency by remaining within the boundary layer. Zhang *et al*. [38] showed that combining micro-V-shaped ribs and dimples further improves heat transfer. Nevertheless, these improvements lead to higher pressure drops, making it essential for future designs to balance heat-transfer enhancement with flow resistance.

D. Pin Fin Cooling

Pin fins are often employed at the turbine blade trailing edge, where high heat loads require increased disturbance. These fins generate wake vortices and promote boundary-layer separation, enhancing heat transfer while also supporting structural integrity. The cooling efficiency depends on fin shape and arrangement. Bhandari [39] found that micro square pin fins with bidirectional stepped height offered superior thermal performance over uniform designs. Kemerli *et al.* [40] demonstrated that shorter rods significantly improve heat transfer, although pressure drops increase. Recent work by Yan *et al.* [41] showed that under rotating conditions, curved pin fins maintain more stable heat-transfer performance than upright or inclined fins. Yeranee *et al.* [42] emphasized that many existing studies are conducted under static conditions, which overlook Coriolis and buoyancy forces that affect flow and temperature distributions during rotation. Consequently, future studies must address pin-fin behavior under rotating conditions and explore their integration with other internal cooling strategies such as ribs, jet impingement, film, and transpiration cooling.

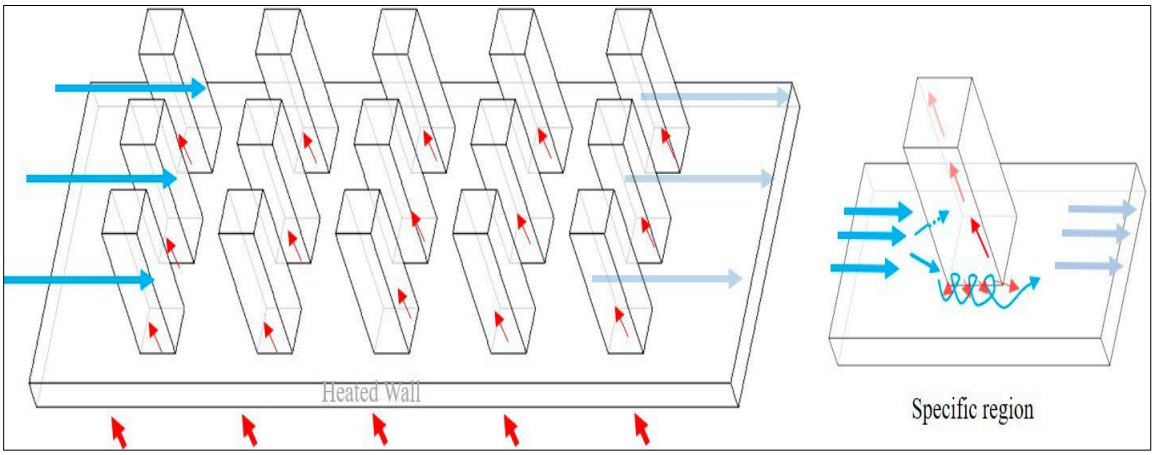

Fig.7 Illustration of Heat Exchange Mechanisms in a Pin-Fin Configuration [43]

III. EVOLUTION AND TRENDS IN COOLING STRATEGIES FOR ULTRA-HIGH TEMPERATURE TURBINE BLADES

At turbine inlet temperatures surpassing 2000 K, future cooling strategies must integrate innovative structures and advanced manufacturing. Figure 9 summarizes key directions.

A. Advanced High-Efficiency Composite Cooling Systems

Composite cooling systems such as impingement–film cooling and double-wall structures with pin fins are vital for improving blade heat resistance and coolant utilization.

1. Impingement–Film Cooling: This method is commonly applied to the leading edge of the blade. Early studies focused on the isolated effects of film or jet cooling, while recent research explores conjugate heat transfer influenced by hole geometry, arrangement, and rotation. Zhang *et al.* [44] showed that smaller film-hole angles and higher mass-flow rates improve cooling efficiency. Singh and Udayraj [45] found that jet impingement significantly affects film-cooling performance, with hole direction and blowing ratio being key parameters. Pu *et al.* [46] proposed a laminated layout for uniform coolant distribution, and Wang *et al.* [47] highlighted Coriolis-force effects under rotation, leading to asymmetric flow and reduced cooling efficiency.

2. Double-Wall Structures with Pin Fins: Double-wall structures with pin fins further boost performance by enhancing heat transfer through jet–fin interaction. Rao et al. [48] showed that pin fins reduce crossflow and improve heat-transfer uniformity. Fan [49] investigated the combined

effects of film holes and pin fins, introducing vortex-enhanced double-wall cooling. These three-part systems offer significant promise, although many influencing factors still require optimization.

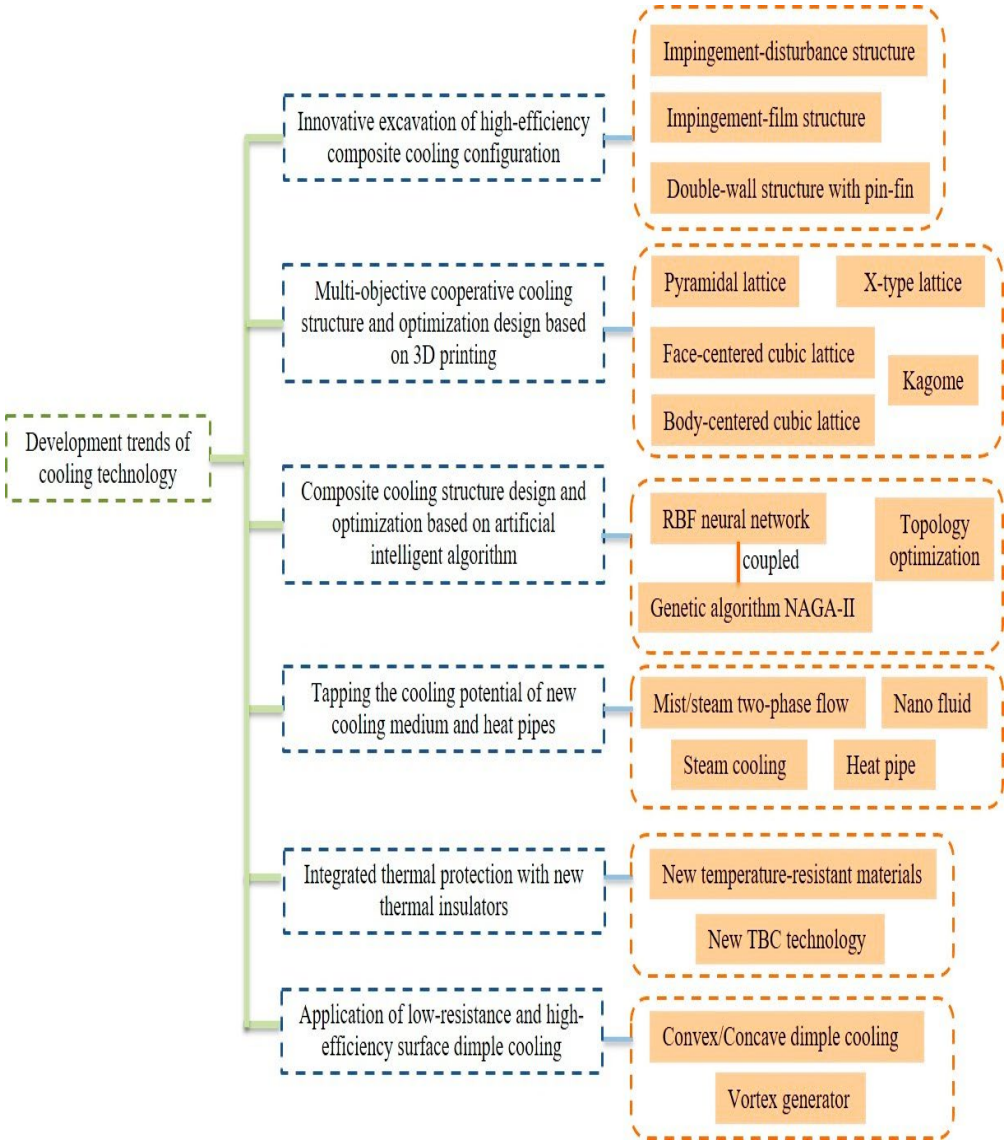

Fig.8 Development Trends of Cooling Technology [44]

Further understanding of flow and heat-transfer mechanisms in these complex configurations is essential for practical application in future blade designs.

B. Multi-Objective Cooling Design via 3D Printing

Additive manufacturing (AM) enables highly integrated designs for thermal, structural, and aerodynamic performance without mold constraints [50], [51]. Siemens has already tested AM-manufactured blades using polycrystalline nickel superalloys at 13,000 rpm and 1250 °C. AM facilitates advanced internal cooling features such as lattice structures, replacing traditional ribs. Ma *et al.* [52] added pyramid lattices to sandwich plates, improving Nusselt numbers by 150%. Xi *et al.* [53] developed X-type truss channels with superior thermal performance. Liang *et al.* [54] found that elliptical FCC lattices offer 27–31% better heat transfer than circular ones, while Wang et al. [55] confirmed the mechanical and thermal superiority of body-centered cubic lattices. Our own work [56], [57] established empirical models linking lattice geometry to both heat transfer and structural integrity. Kagome structures (Figure 10) are also emerging as promising AM-enabled cooling geometries. Yang *et al.* [58] demonstrated higher heat transfer than tetrahedral lattices, albeit with increased pressure drop. Shen *et al.* [59], [60] reported 26–31% better heat performance for Kagome structures compared to wire-woven panels. Sarwesh *et al.* [61] showed that Kagome-based microchannels outperform smooth channels by a factor of 3–6 in heat transfer. These AM-fabricated lattice structures enable multifunctional optimization of cooling systems by combining thermal efficiency with strength, weight reduction, and aerodynamic performance, making them highly promising for next-generation turbine blades.

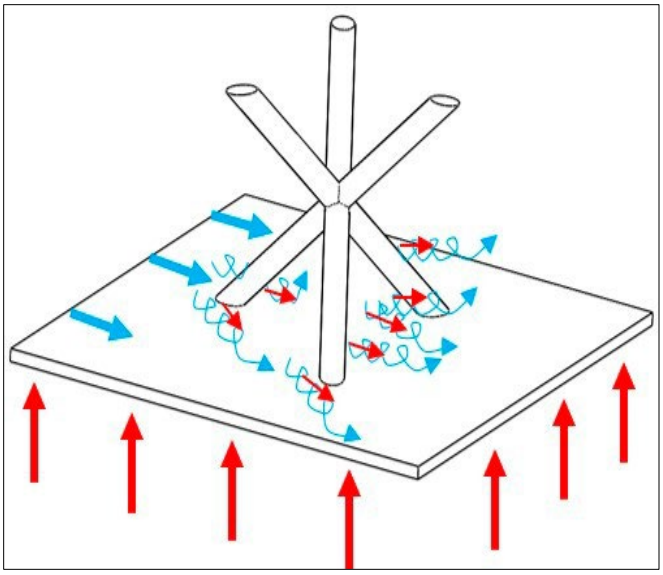

Fig.9 Schematic Diagram of Heat Exchange from Kagome Structure [58]

C. Design and Optimization of Composite Cooling Structures Using AI Algorithms

The optimal design of composite cooling structures involves a deep understanding of the underlying elements, including the objective function, design variables, and constraints. Engineering practice often requires multi-objective optimization, necessitating the careful selection of optimization strategies for both parameter and shape optimization. The design process typically begins by creating a design database, which forms the foundation for assessing the cooling performance of various configurations. Numerous studies have explored the influence of geometric parameters on the performance of composite cooling structures, with optimization methods ranging from Kriging surrogate models to topology optimization. The following table summarizes some of the key optimization techniques and their applications in composite cooling-structure design.

TABLE IV SUMMARY OF OPTIMIZATION TECHNIQUES FOR COMPOSITE COOLING STRUCTURES

Study	Optimization Method	Key Design Parameters	Model/Method Used	Main Outcomes
[62]	Kriging Surrogate Model	Impingement hole pitch, hole diameter, channel height, film hole diameter	CFD simulations, variance analysis	Identified key design parameters influencing cooling performance
[63]	Agent-based Prediction Model	Geometric configuration and cooling efficiency	Radial Basis Function (RBF) neural network, Latin Hypercube Sampling, NAGA-II genetic algorithm	Optimal design solution for composite cooling structures
[64]	Multiscale Topology Optimization	Material distribution in lattice structures	Topology optimization for lattice structures	Enhanced cost-effectiveness and efficiency in lattice structure design
[65]	Topology Optimization	Lattice structure design for improved material distribution	Topology optimization	Significant improvements in compressive, flexural, and energy absorption properties
[66]	Density-based Topology Optimization	Cooling channel design under turbulent flow conditions	Density-based topology optimization	Enhanced thermal performance, improved temperature uniformity, and reduced pressure drop

This table provides an overview of various optimization techniques applied to composite cooling structures, highlighting the key parameters, methods used, and the outcomes achieved in each study. It showcases how different approaches-including surrogate modeling, neural networks, and topology optimization-are employed to increase the thermal and structural efficiency of cooling channels and lattice structures. These innovations offer promising strategies for improving the overall efficiency and effectiveness of cooling systems in engineering applications.

D. Integrated Thermal Protection with Advanced Insulators

Current turbine blade materials primarily consist of nickel- and cobalt-based superalloys, which have reached a mature stage of development. To further enhance performance, trace alloying and advanced thermal barrier coatings (TBCs) are employed. TBCs consist of a ceramic top layer with low

thermal conductivity and a metallic bond coat that mitigates thermal stresses resulting from mismatched thermal-expansion coefficients. TBCs significantly improve the thermal efficiency of turbine blades. Pu *et al.* [67] investigated TBC effects on double-wall cooling structures and concluded that TBC thickness had a more substantial impact than simply increasing cooling-air mass flow. While thicker coatings improve insulation, they may also suffer from thermal degradation and undermine the positive effects of additional cooling airflow.

Ceramic matrix composites (CMCs) are gaining interest due to their high-temperature strength and lightweight characteristics, making them ideal candidates to replace metallic alloys in aerospace applications [68]. With a typical 250-µm TBC, surface temperatures can be reduced by 380–440 K under conventional cooling [69].

Yttria-stabilized zirconia (YSZ) is the most widely utilized ceramic for TBCs, with performance-enhancing dopants such as Sc, La, Al, and Ni. Mitsubishi Heavy Industries (MHI) has developed pyrochlore-structured $A_2B_2O_7$ TBCs that support turbine operation at up to 1850 K. GE and Siemens have already integrated advanced TBCs into their turbine designs. For instance, GE's 7/9HA series features directionally solidified, single-crystal blades with next-generation TBCs [70].

Siemens' H-series and HL-series turbines employ crystalline materials with modular, high-performance TBC systems. Integrated thermal protection combining advanced CMCs and high-performance TBCs represents a passive thermal-management strategy that complements or outperforms active cooling under extreme conditions. Exploiting these technologies is essential to surpass the 2000 K turbine inlet temperature threshold.

E. High-Efficiency Cooling via Low-Resistance Dimpled Surfaces

Combining multiple cooling techniques can synergistically enhance thermal performance. Incorporating surface texturing-particularly via dimples-is considered the third pillar of cooling enhancement due to its ability to disrupt boundary layers and generate vortices that improve convective heat transfer. Traditionally, rectangular groove surfaces have been used. Zontul *et al.* [71] conducted experiments and CFD simulations on rectangular-groove channels using the standard k–ε turbulence model for Reynolds numbers ranging from 2000 to 6500.

Their findings showed that groove channels achieved 1.9–2.4 times higher Nusselt numbers than smooth channels, albeit at the cost of increased pressure drop. Dimpled surfaces offer a novel alternative with superior thermal efficiency. Ahmed *et al.* [72] demonstrated that heat sinks with eight convex/concave dimples significantly extended the uniform operating temperature duration for a solar panel system. Qi *et al.* [73] compared various jet-impingement target surfaces and concluded that convex dimples offered superior heat transfer, whereas concave dimples incurred lower pressure losses. Dimple cooling is often enhanced using vortex generators. Jeong *et al.* [74] studied crescent-shaped vortex generators positioned downstream of dimples, while Yang *et al.* [75] proposed upstream wedge-shaped vortex generators. In both cases, flow mixing and heat transfer were significantly improved. These configurations demonstrated better thermohydraulic performance compared to conventional dimple structures. In summary, surface-dimple cooling-especially when combined with vortex generators-offers a low-resistance, high-efficiency strategy well suited for advanced thermal-management systems in turbine applications.

IV. MIST-ASSISTED COOLING

Mist-assisted cooling involves injecting fine water droplets into the coolant airstream, where they act as distributed heat sinks. These droplets evaporate progressively, absorbing heat from the surrounding air and turbine blade surfaces. The resulting two-phase cooling significantly lowers blade temperature, especially near stagnation regions and downstream zones where conventional air cooling becomes less effective. Unlike spray cooling, which uses high-pressure jets and risks surface flooding, mist cooling employs a low droplet concentration suspended in air, allowing droplets to follow streamlines without direct wetting. This method offers enhanced thermal protection through both convective and evaporative mechanisms.

Advantages Include:

1. Enhanced cooling performance through localized evaporation
2. Flexibility in adjusting mist concentration, droplet size, and distribution
3. Compatibility with advanced coatings and high-temperature materials
4. Environmental benefits due to water-based coolant use

Challenges Include:

1. Droplet coalescence leading to unintended "water cooling" along surfaces
2. Corrosion risks from moisture exposure
3. Potential clogging from impurities in the coolant
4. Added system complexity, energy consumption, and maintenance demands
5. Due to these trade-offs, mist-assisted cooling remains largely at the research stage, with limited commercial deployment.

However, based on experimental studies, a generalized system architecture includes the following components:

1. Coolant delivery system with reservoirs, pipelines, and high-pressure pumps
2. Atomization unit to generate fine mist from pressurized coolant
3. Mixing chamber with baffles for uniform mist–air blending

4. Strategic injection ports near blades or vanes to target high-heat zones
5. Sensors and control systems to monitor and regulate mist flow, pressure, and distribution

While promising, further development is necessary to ensure reliability and integration into commercial gas turbine platforms.

A. Performance of Mist-Assisted Jet Impingement Cooling

Mist-assisted cooling performance hinges on several interacting parameters, each influencing evaporation dynamics, heat-transfer augmentation, and downstream coverage. Table V summarizes the key variables, their typical ranges, and their primary effects on cooling effectiveness, based on the experimental studies by Li *et al.* [76].

B. Contextual Overview

In mist-assisted jet impingement, fine droplets act as evaporative heat sinks, markedly boosting local Nusselt numbers and extending effective cooling downstream where single-phase air fails. Optimal performance occurs with moderate mist loading (1–2%), fine droplet sizes (<30 μm), and well-tuned jet configurations.

Slot jets, while less effective in pure steam, excel when carrying mist by delivering more uniform film coverage. Designers must balance increased complexity-such as mist generation and droplet control-with the substantial gains in surface protection, especially under high heat-flux regimes.

TABLE V KEY PARAMETERS IN MIST-ASSISTED JET IMPINGEMENT COOLING

Parameter	Definition	Typical Range	Effect on Cooling Performance	Reference
Mist Loading Fraction (f)	Mass fraction of water in the coolant stream	0.75 % – 3.5 %	Increases the local heat-transfer coefficient; at 1.5% *f*, approximately 200% enhancement occurs at stagnation, and higher *f* shifts the peak downstream	[77]
Droplet Diameter (d_p)	Sauter mean diameter of injected droplets	10 – 50 μm	Smaller droplets evaporate faster, improving both local and downstream cooling, whereas larger droplets prolong the evaporative sink	[65, 43]
Reynolds Number (Re_p)	Jet Reynolds number based on hole diameter and jet velocity	7 500 – 22 500	Higher Re_p increases jet penetration and mixing; the relative enhancement from mist is more pronounced at lower Re_p	[78]
Surface Heat Flux (q″)	Heat load applied to the target surface	3.3 – 13.4 kW/m²	Lower q'' yields larger percentage gains (up to 400%); at high q'', absolute heat removal still increases significantly	[49]
Injection Configuration	Discrete jets vs. slot nozzles	Row of 1–5 holes or slot jets	In steam-only flow, discrete jets outperform slots; in mist–steam flow, slots provide more uniform coverage and cooling	[58]
Nozzle-Plate Confinement Ratio	Ratio of nozzle diameter to nozzle-to-plate spacing	0.5 – 1.0	Higher confinement focuses the jet, enhancing stagnation cooling; lower confinement promotes a wider spread of mist	[78]

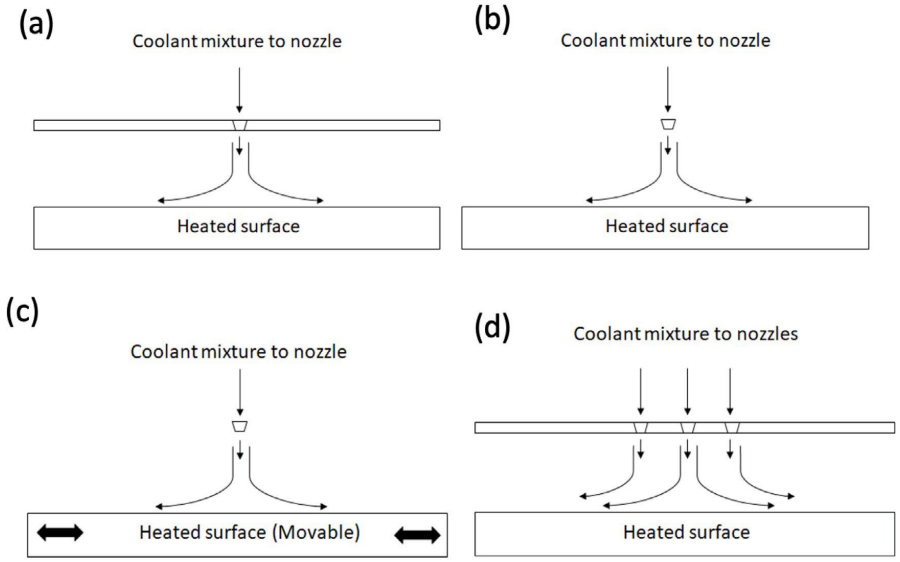

Fig.10 Schematic Illustration of Mist-Assisted Jet Impingement Configurations on a Flat Surface: (a) Confined Jet with One or Multiple Nozzles, (b) Unconfined Jet with One or Multiple Nozzles, (c) Unconfined Jet with Three Nozzles [79]

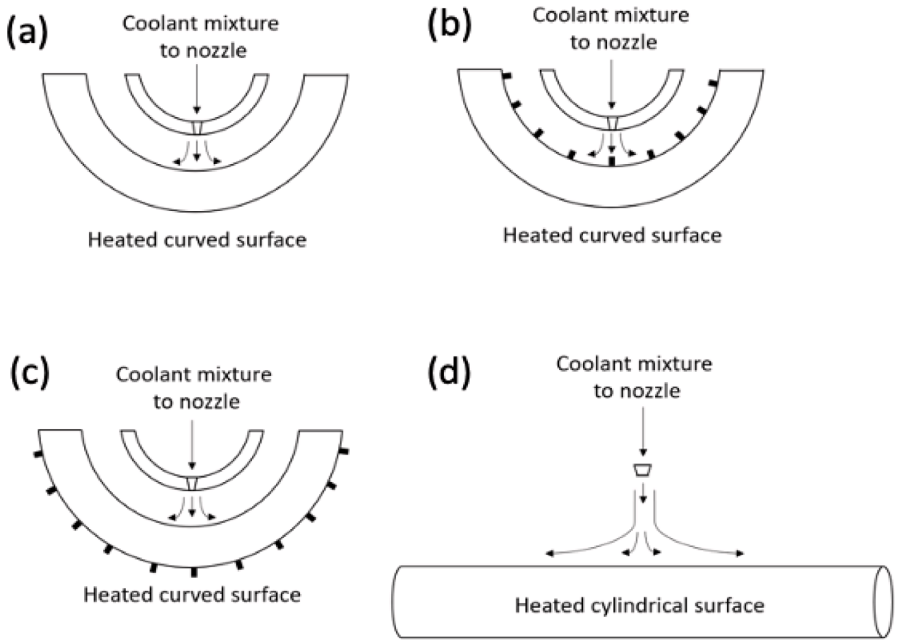

Fig.11 Schematic Illustration of Mist-Assisted Jet Impingement Configurations on Curved Target Surfaces Using a Confined Jet: (a) Concave Surface, (b) Concave Surface Featuring Ribs, (c) Convex Surface Featuring Ribs [80]

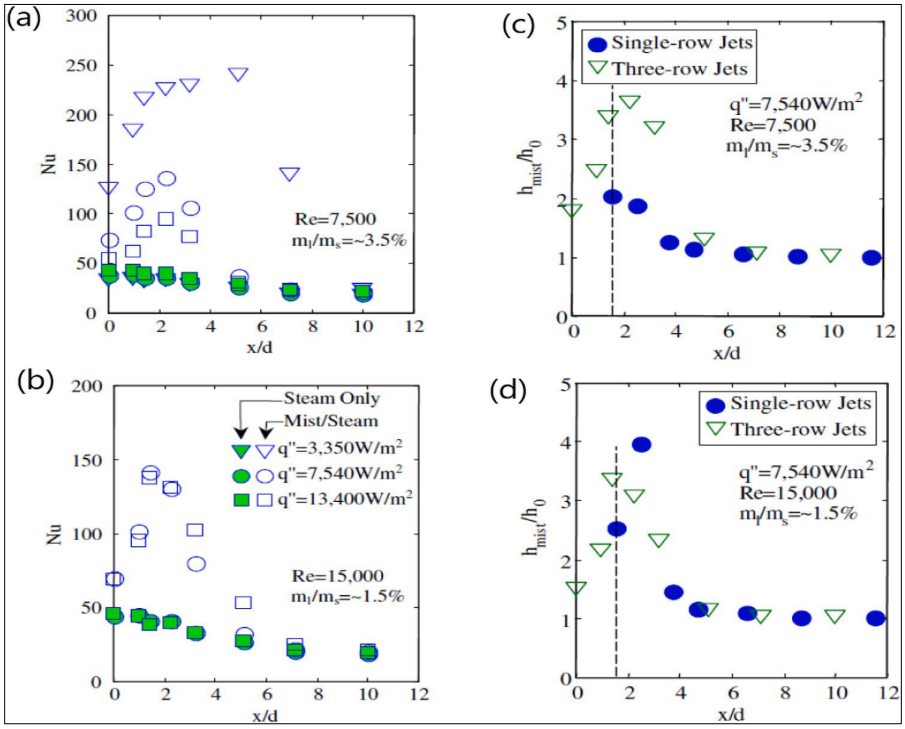

Fig.12 Nusselt Number Comparison for Single-Phase Steam Versus Two-Phase Mist-Assisted Steam Jet Impingement Cooling At *Rep* of 7500 (a) And 15000 (b). Heat Transfer Enhancement for Single-Row and Three-Row Round-Hole Configurations Under Mist-Assisted Steam Cooling at *Rep* of 7500 (c) And 15000 (d) [81].

C. Mist Assisted Jet Impingement Cooling of Curved Surface

Li *et al.* [82] experimentally investigated mist-assisted steam impingement cooling on both concave and flat surfaces using a slot-jet configuration. Results revealed that the maximum heat-transfer enhancement occurs slightly off the jet centreline, with significant cooling observed at the stagnation point for both geometries. Introducing a small mist fraction (≤0.5%) into the coolant notably reduced surface temperatures near the stagnation region compared to the dry-steam case. At the stagnation point, heat-transfer coefficients improved by 30% to 200%, with greater enhancement observed at lower surface heat fluxes (q''), particularly for curved surfaces.

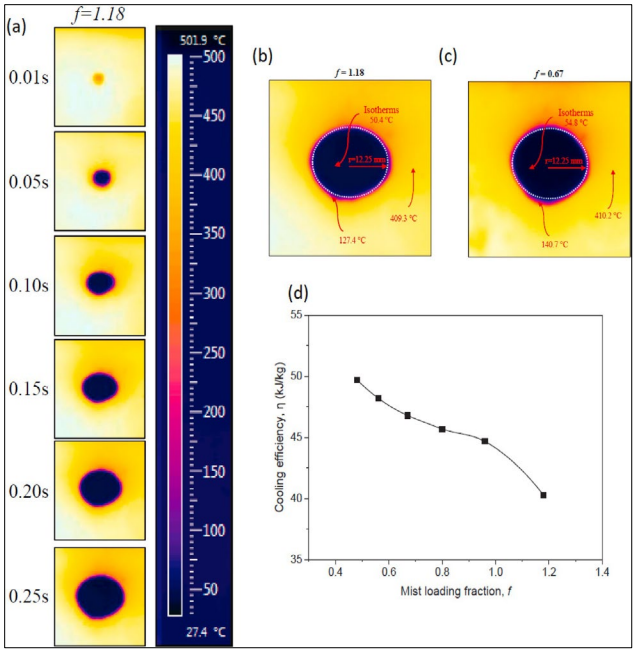

Fig.13 Infrared Thermal Images of Transient Hot Surface Cooling: (a) At Different Times For f = 1.18, (B–C) At t = 0.25 S For f = 1.18 And 0.67, (D) Cooling Efficiency Variation With f.

D. Emerging Trends and Future Directions in Mist-Assisted Jet Impingement Cooling Technology

The following points summarize the current understanding and future research directions for mist-assisted jet impingement cooling:

1. Extensive parametric studies have explored the effects of nozzle geometry, droplet size, and mist flow rate on cooling performance. However, a comprehensive understanding of the underlying two-phase flow mechanisms remains limited due to restricted access to high-resolution simulation data and low-uncertainty, non-intrusive experimental techniques.
2. Nozzle design is essential for enhancing atomization quality and mist distribution. Improved atomization can enhance droplet uniformity and heat-transfer performance.
3. While current research demonstrates promising cooling potential, combining mist-assisted cooling with other advanced techniques may yield further improvements in thermal management.
4. Most existing studies focus on simplified or idealized configurations. Future work should emphasize realistic geometries and operating conditions to validate the practical applicability of this technique in actual gas turbine systems.

E. Experimental Studies on Mist-Assisted Film Cooling

Experimental investigations have demonstrated that adding a small mist fraction to film-cooling air significantly boosts local and downstream cooling effectiveness across various hole geometries and blowing ratios.

TABLE VI COMPARISON OF EXPERIMENTAL STUDIES ON MIST ASSISTED FILM COOLING

Study	Surface / Holes	Mist	Key Metrics	Highlights
[84]	Flat plate / multiple holes	0 – 1.4 M	Net η increase: up to +190 % (local) Coverage ↑83 % at M=0.6	Optimal at M≤0.6; mist and air jets detach at higher M
[85]	Flat plate / multiple holes	similar range	17 % droplets overshoot η peaks at “bend-back”	Droplet–air momentum mismatch; enhanced cooling where droplets re-approach surface
[73]	Flat plate / fan & cyl holes	low M	η enhancement: +40 % (near hole) +170 % downstream	Fan holes yield wider coverage and higher η than cylindrical at low M
[77]	Flat plate / cylindrical	up to 2.1 %	η↑26 % max Coverage peaks at M=1.11	Max η at intermediate M; jet lift-off at M≈0.6
[86]	Facility development	various d_p	Measurement uncertainty vs. d_p	Smaller droplets follow flow better but vanish above ~5 µm; larger droplets improve elevation

Mist-assisted film-cooling experiments consistently demonstrate that introducing a controlled fraction of water droplets into the coolant stream can markedly improve both local and downstream cooling effectiveness. Across a range

of hole geometries-from cylindrical to fan-shaped-and blowing ratios, researchers have observed net effectiveness gains of up to 200% at optimal mist loadings. These studies also highlight critical phenomena such as droplet overshoot, jet lift-off, and reattachment ("bend-back") that govern where and how mist enhances the film layer.

F. Numerical Studies on Mist-Assisted Film Cooling

1.Flat-Surface Mist-Assisted Film Cooling with One Coolant Hole: CFD simulations confirm that optimal droplet size and mist concentration are critical for maximizing film-cooling enhancement, with performance strongly tied to hole shape, jet–crossflow interactions, and surface geometry. Complementary CFD investigations validate and extend these experimental insights, revealing the interplay between droplet size, concentration, and jet–crossflow dynamics in mist-enhanced film cooling. Simulations show that sub-10 µm droplets at 2–5% loading yield the greatest cooling gains, whereas larger droplets or excessive mist can diminish performance. Furthermore, numerical models help pinpoint optimal hole shapes and operating conditions for real turbine geometries.

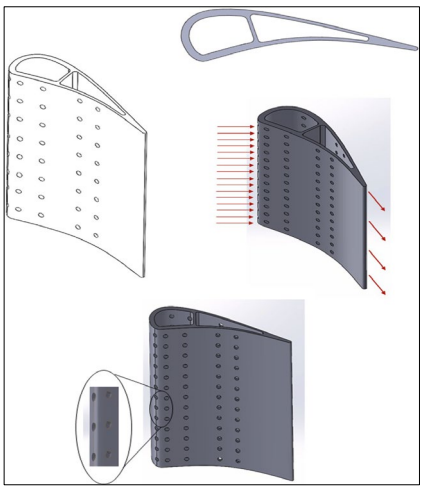

Fig.14 Schematic Representation of Mist-Assisted Film Cooling on a Curved Surface Featuring Multiple Holes, Illustrated from Various Perspectives [87]

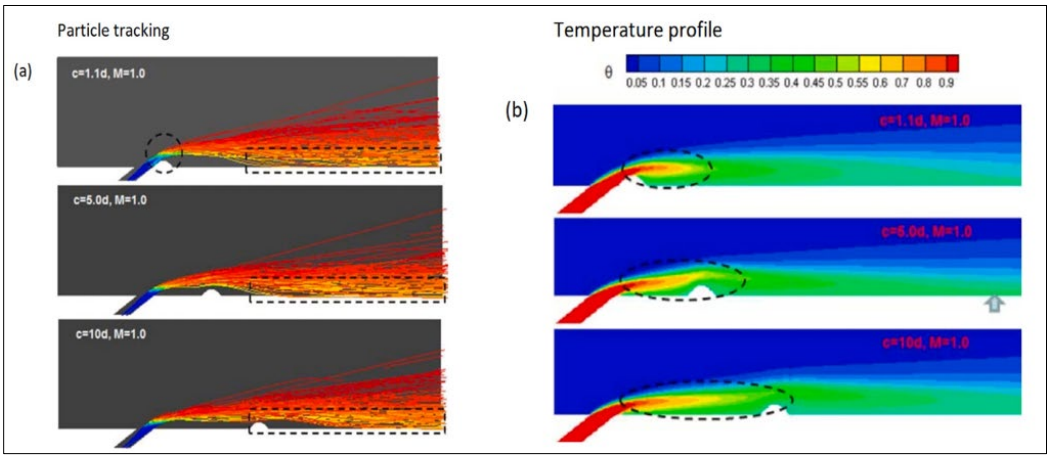

Fig.15 Influence of Plate Deposition Location On (a) Droplet Particle Tracking and (b) The Resulting Dimensionless Temperature [88]

TABLE VII NUMERICAL STUDIES ON SINGLE COOLANT HOLE

Study	Hole Type	Mist	Key Metrics	Highlights
[88]	Round & fan-shaped	2 % concentration	η↑30 % avg; spanwise peak +50 % d_p: 5→20 µm causes η drop from +43 % to +5 %	Best at $d_p \leq 10$ µm and M≈0.66; effectiveness drops at higher d_p and M
[89]	Round	up to 7 %	η↑40.7–76.3 % at 2–5 % mist; peak η+65.1 % at 7 % mist	Optimal at 5 % mist and $d_p \approx 10$ µm; small droplets move inward, large droplets move outward
[85]	Conducting wall	up to 8 %	High-temperature area shrinks with mist concentration	Effective in eliminating mid-hub hot spots at 8 % mist

A computational study on mist-assisted film cooling using a conducting wall representative of heavy-duty gas turbine blades was performed by [90] (Fig. 17). The study demonstrated that the extent and location of enhanced cooling are highly dependent on droplet diameter (d_p). Temperature contour plots (Fig. 16) at the suction and pressure sides showed elevated surface temperatures near the mid-hub region under dry-air conditions. However, the addition of mist significantly mitigated this thermal hotspot. At a mist concentration of 8%, the high-temperature region became negligible, confirming the effectiveness of mist cooling in reducing localized surface heating.

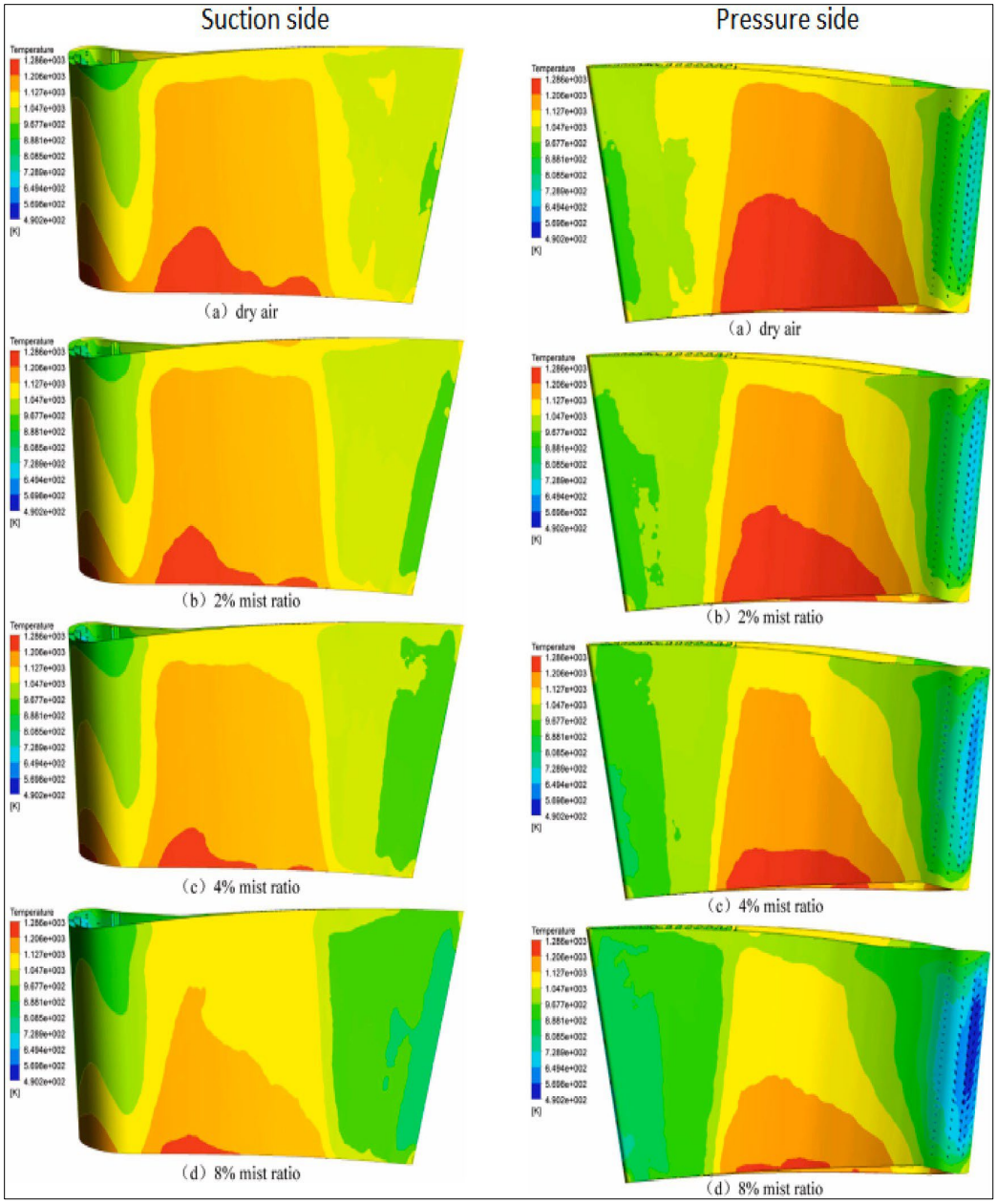

Fig.16 Influence of Mist Concentration on the Surface Temperatures of the Suction and Pressure Sides [90]

G. Potential Developments in Mist-Assisted Film Cooling

Based on the current state of research, several key opportunities exist to further enhance the performance and applicability of mist-assisted film cooling:

1. While current studies highlight the impact of coolant-hole geometry on cooling performance, further investigation is needed to optimize hole arrangement, spacing, and orientation. Future work should aim to improve not only cooling effectiveness but also surface-temperature uniformity and coolant coverage for enhanced thermal management.
2. As findings suggest that smaller droplets and higher mist concentrations improve heat transfer, innovative techniques to generate, control, and characterize fine mist with consistent size distribution should be developed. Experimental setups and simulation approach capable of accurately handling high droplet concentrations at small diameters warrant further exploration.
3. To move from laboratory experiments toward field deployment, research should increasingly focus on realistic turbine geometries and operating conditions. Advances in high-fidelity simulations and non-intrusive measurement technologies can facilitate this transition and improve predictive accuracy under extreme environments.
4. Although mist forms an effective thermal barrier, high mist concentrations may pose a corrosion risk to turbine components. Future studies should investigate long-term material durability and develop high-performance alloys

and coatings that withstand thermal, mechanical, and chemical stresses in mist-laden environments.

V. TBC COOLING TECHNIQUE

A. Key Studies on TBC Cooling Techniques

Rising turbine inlet temperatures in gas turbines, driven by efficiency demands, have exceeded material limits, necessitating thermal barrier coatings (TBCs) since the 1970s. Early TBCs employed yttria-stabilized zirconia (7–8YSZ) topcoats over metallic bond coats to insulate components such as combustors and blades. In the 1980s–1990s, Air Plasma Spraying (APS) and Electron Beam Physical Vapor Deposition (EBPVD) emerged, with APS suited for combustors and shrouds and EBPVD preferred for blades due to its strain-tolerant columnar structure. Research in the 1990s clarified TBC structures-bond coats, ceramic topcoats, and the thermally grown oxide (TGO) layer formed during operation-and focused on the TGO's impact on durability. By the 2000s, TBCs combined with film cooling enabled higher operating temperatures, improving efficiency and component life. Modern challenges include managing TGO growth and spallation, with ongoing research optimizing TBCs for complex turbine geometries.

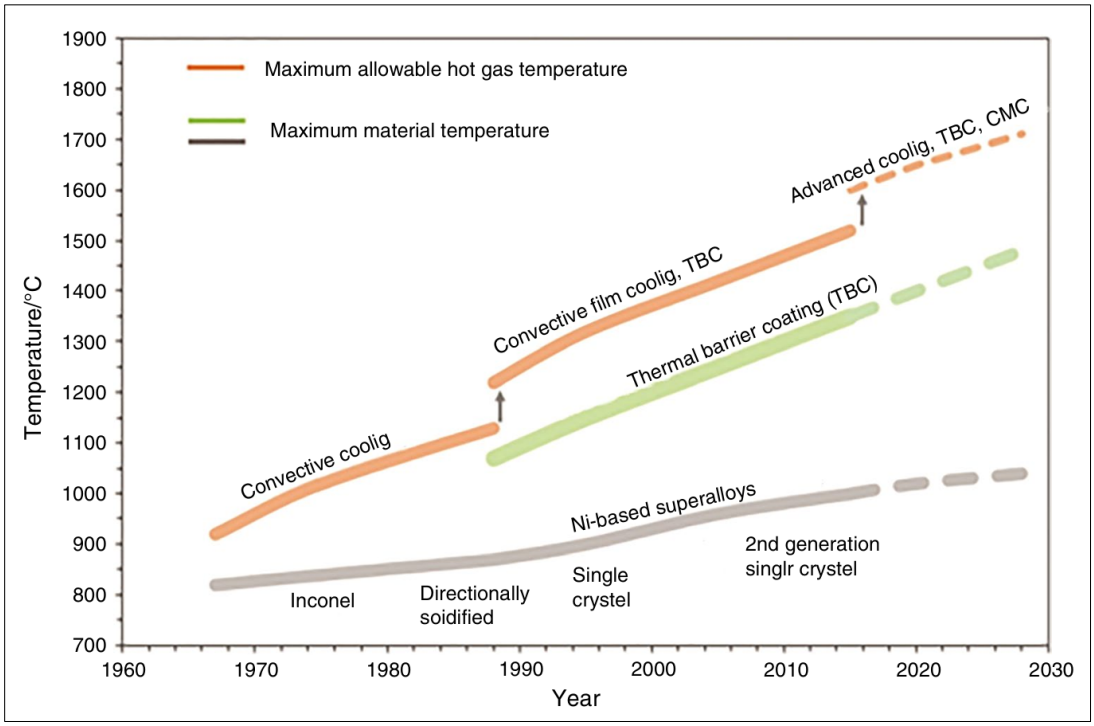

Fig.17 Trends in Turbine Cooling Techniques with Increasing Inlet Temperature [91]

The following table summarizes pivotal studies and findings on TBC-assisted cooling techniques, providing a concise reference for their development and application in gas turbines. The evolution of TBC-assisted cooling techniques has been instrumental in enabling gas turbines to operate at elevated temperatures, thereby boosting efficiency and extending component life.

From the early adoption of YSZ-based coatings to the development of sophisticated deposition methods such as APS and EBPVD, TBCs have transformed turbine design. Ongoing research continues to address challenges such as TGO growth and coating durability, facilitating further innovation in gas turbine technology. Conventional film cooling (FC) exhibits limitations, including kidney-shaped vortex pairs that draw hot mainstream flow toward the wall, coolant-jet separation at high injection ratios (IR > 1), and poor spanwise coolant distribution, as noted by Harrison *et al.* [12], Khalatov *et al.* [13], and Schreivogel *et al.* [95]. Trenched film cooling (TFC) mitigates these issues by reducing jet detachment at high IR, minimizing vortex intensity, and enhancing spanwise film-cooling effectiveness (FCE) [96].

TABLE VIII KEY STUDIES ON TBC COOLING TECHNIQUES

Reference	Year	Focus Area	Key Findings	Deposition Method	Component Application
[92]	1978	TBC Material Selection	Established 7YSZ as a thermally stable topcoat material with low thermal conductivity.	APS	Combustor, Blades
[56]	1980	TBC System Design	Introduced multilayer TBC with bond coat and ceramic topcoat for enhanced insulation.	APS	Combustor
[59]	1985	TGO Formation	Identified TGO as a critical layer affecting TBC adhesion and durability.	APS, EBPVD	Blades, Vanes
[93]	1990	TGO Growth Mechanisms	Analyzed TGO growth dynamics and its impact on TBC lifespan under thermal cycling.	EBPVD	Blades
[38]	1995	TBC Degradation	Highlighted TGO-induced spallation as a key failure mechanism in TBC systems.	APS, EBPVD	Combustor, Blades
[74]	2000	Bond Coat Optimization	Demonstrated improved adhesion through optimized bond coat compositions.	EBPVD	Vanes
[39]	2005	APS Deposition	Confirmed APS as cost-effective for thick TBC coatings on stationary components.	APS	Combustor, Shrouds
[89]	2008	APS Advancements	Improved APS techniques for enhanced coating porosity and thermal resistance.	APS	Combustor
[94]	2010	EBPVD for Blades	Highlighted EBPVD's columnar microstructure for better strain tolerance in blades.	EBPVD	Blades, Vanes
[48]	2012	EBPVD Optimization	Optimized EBPVD for improved thermal shock resistance in high-pressure turbines.	EBPVD	Blades
[25]	2015	TBC-Film Cooling Synergy	Demonstrated enhanced cooling efficiency through TBC integration with film cooling.	APS, EBPVD	Blades, Combustor

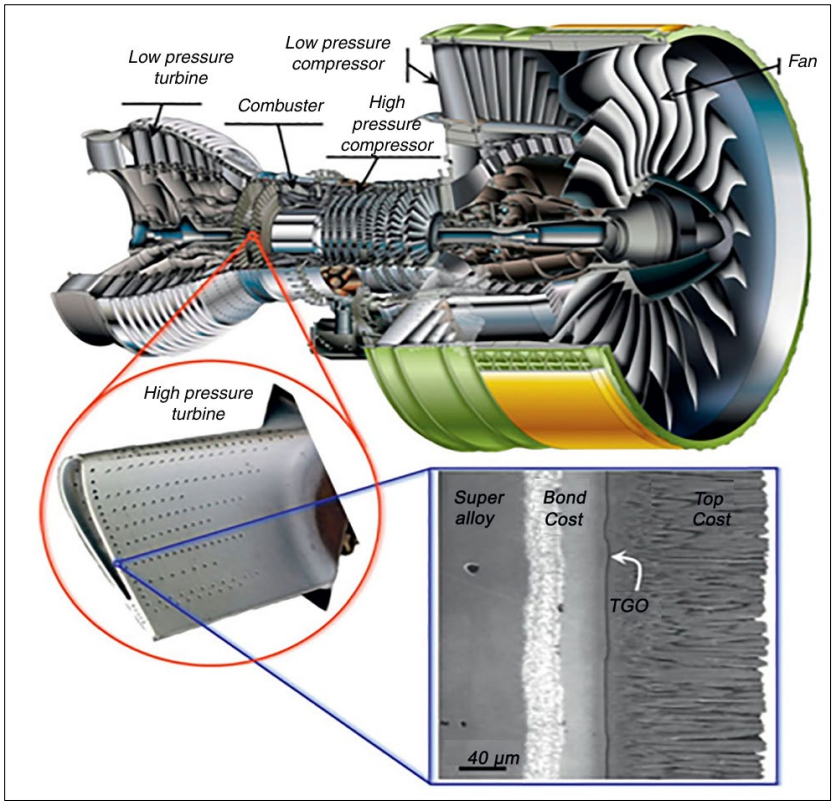

Fig.18 Cutaway View of a Turbofan Engine, Highlighting the High-Pressure Turbine Equipped with a Thermal Barrier Coating [94]

Cratered surfaces increase spanwise-averaged FCE by 50% compared to non-cratered models [97], while ramp-assisted FC achieves two to three times higher FCE than non-ramped designs [98]. Surface modifications such as slots, indents, and protrusions improve FC on the leading edges, pressure and suction sides, end walls, and flat surfaces of gas turbine components. Computational fluid dynamics (CFD) is widely used to evaluate the performance of these cooling methods.

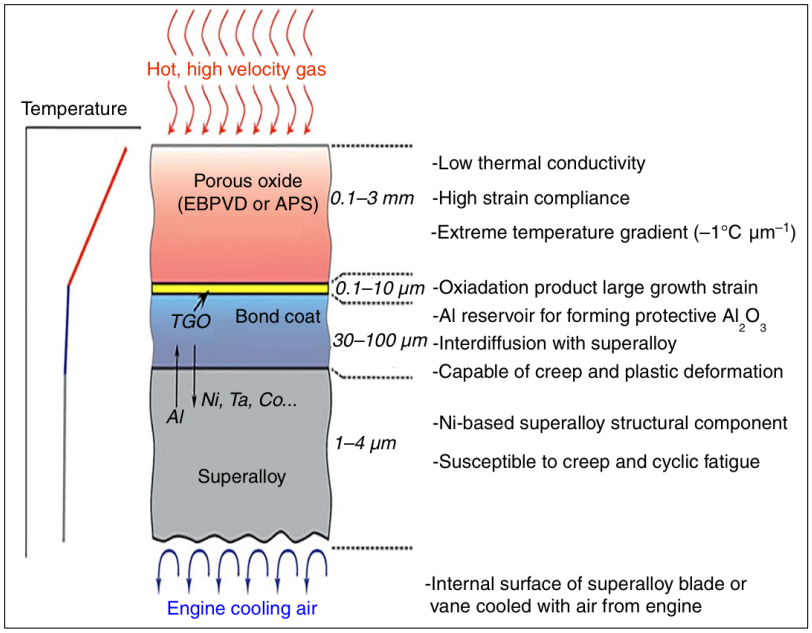

Fig.19 Blade Cooling Composite Structure [97]

Thermal barrier coatings (TBCs) are essential for protecting gas turbine components from extreme temperatures, enabling higher turbine inlet temperatures and enhancing engine efficiency. Feuerstein *et al.* [99] detail key TBC coating techniques, including plasma spray and electron beam physical vapor deposition (EBPVD) for the ceramic topcoat, and shrouded plasma spray and high-velocity oxygen fuel (HVOF) for the bond coat. Bond-coat materials such as MCrAlY, diffusion aluminide, and platinum aluminide ensure adhesion and oxidation resistance. While EBPVD offers superior performance for turbine blades, its equipment cost approaches 50% of the total expense, whereas plasma spray is more economical but incurs higher material and labor costs. TBCs extend component service life twofold, provide auto-toughening effects, and shield against high-temperature environments, although prolonged exposure can cause spallation due to thermally grown oxide (TGO) formation, highlighting the bond coat's multifunctional role.

TABLE IX TBC AND SURFACE-MODIFIED FC OVERVIEW

Aspect	Details	Numeric Data	Key Findings	References
TBC Temperature Protection	Protects components from high temperatures	Up to 1500°C	Enables higher turbine inlet temperatures	[100]
Service Life Extension	Extends component durability	100-200% increase	Reduces maintenance frequency and costs	[97]
Coating Technique Costs	EBPVD vs. Plasma Spray comparison	EBPVD: ~50% equipment cost, Plasma Spray: 20-30% higher material costs	Trade-off between initial investment and operational expenses	[101]
Surface-Modified FC Types	Slot: Holes in grooved slots, Indent: Holes in depressions, Protrusion: Holes near raised surfaces	20-50% FCE improvement	Enhances cooling efficiency and component longevity	[102]
Compound Angle FC	Angled injection for improved coverage	~30% increase in lateral coolant spread	Improves film uniformity and effectiveness	[103]
Geometric Parameters	Hole diameter: 0.5-2 mm, Spacing: 3-6 diameters, Slot width: 1-3 mm	Influences coolant distribution	Optimizes cooling performance	[85]
Flow Parameters	Blowing ratio: 0.5-2.0, Reynolds number: 10,000-50,000	Affects jet penetration and mixing	Critical for FC design and efficiency	[104]
Measurement Techniques	Infrared thermography, heat flux sensors, flow visualization	Accuracy within ±5%	Validates performance and supports design improvements	[105]

VI. STATE-OF-THE-ART THERMAL MANAGEMENT STRATEGIES FOR GAS TURBINES

Turbine cooling research began in the early 2010s with a focus on innovative approaches aimed at improving the efficiency and longevity of gas turbine components. In 2013, a pioneering study introduced the Micro Tangential Jet (MTJ) scheme, which featured secondary jets flowing parallel to the vane surface. This design significantly improved cooling uniformity and achieved a net heat flux reduction (NHFR)

exceeding 100% in critical regions, outperforming traditional louver designs and laying the groundwork for future advancements in film cooling [106]. By 2018, the research focus had shifted toward more comprehensive system analyses. Researchers developed mathematical models for energy and exergy analysis of air film-cooled gas turbine cycles, incorporating radiative heat transfer. Their findings revealed that traditional models had underestimated coolant requirements by 5–6% due to neglecting radiative heat flux, providing a more accurate approach to cooling predictions and emphasizing the combustor as the primary source of irreversibility.

In 2024, two significant studies advanced the field further. One study combined experimental and numerical methods to investigate jet-impingement cooling within rib-roughened concave passages for leading-edge cooling [107]. The addition of V-shaped ribs produced a marked increase in local Nusselt numbers, particularly under high-crossflow conditions, demonstrating the potential of ribbed designs for internal cooling. Meanwhile, another study quantified the contribution of radiative heat flux on film-cooled plates, finding that radiation could account for up to 50% of the total heat flux at high temperatures, thereby refining cooling-performance predictions [108]. The year 2025 marked a period of prolific advancements. One study used high-fidelity CFD to examine the effects of water vapor concentration on film-cooling effectiveness in hydrogen-fired turbines. It reported that higher water vapor fractions reduced cooling performance due to increased specific heat, offering important insights into hydrogen-combustion environments.

Another breakthrough came with a novel shelf squealer tip design featuring a rim opening, which achieved a 93.2% reduction in net heat flux and an 8.1% decrease in pressure loss, demonstrating the substantial benefits of simple geometric modifications. Efficiency in modeling also improved with the introduction of the Equivalent Boundary

Model (EBM) in 2025. The EBM reduced grid requirements by 20–38% and simulation time by approximately 30%, offering an optimal trade-off between precision and computational efficiency for rapid design optimization. Additionally, a Low Order Model (LOM) for transpiration-cooled nickel blades was developed, coupling aerothermal predictions with crystal-plasticity finite element modeling to lower metal temperatures and stresses while mapping fatigue regimes [109].

TABLE X TURBINE COOLING TECHNOLOGIES

References	Year	Key Technology/Method	Main Findings
[110]	2013	Micro Tangential Jet (MTJ) scheme	Superior cooling uniformity, NHFR > 100% in key regions
[95]	2018	Energy and exergy analysis with radiative heat transfer	Traditional models underestimate coolant needs by 5–6%
[101]	2024	Jet impingement cooling with V-shaped ribs	V ribs boost local Nusselt numbers, optimal with high crossflow
[102]	2024	High-temperature radiation characteristics	Radiation accounts for up to 50% of total heat flux
[103]	2025	Effects of water vapor on film cooling	Higher water vapor reduces η due to increased c_p
[111]	2025	Shelf squealer tips with rim opening	93.2% reduction in net heat flux, 8.1% lower pressure loss
[112]	2025	Equivalent Boundary Model (EBM)	Reduces grid requirements by 20–38%, simulation time by ≈30%
[105]	2025	Low Order Model (LOM) for transpiration cooling	Reduces metal temperatures and stresses, maps fatigue regimes
[113]	2025	Laterally non-symmetrical fan-shaped holes	18.6% reduction in uncooled area, 70.7% less secondary flow deviation
[114]	2025	Multi-cavity slashface gap design	Superior protection at higher blowing ratios, redirects coolant effectively

Further innovation came with a study on laterally non-symmetrical fan-shaped holes near the endwall of low–aspect–ratio vanes. This configuration reduced uncooled areas by up to 18.6% and secondary-flow deviation by 70.7%, highlighting the advantages of asymmetric hole designs.

Finally, a multi-cavity slash-face gap design was explored, redirecting coolant to critical downstream regions and enhancing cooling protection at higher blowing ratios, marking a sophisticated step in endwall cooling.

A. Advanced Geometric and Computational Strategies for Turbine Thermal Control

In 2024, scientists embarked on a quest to improve gas turbine cooling. Kim, using pressure-sensitive paint, enhanced film-cooling effectiveness by 5.1% with a small leeward fillet. His further research confirmed its success and cautioned against windward modifications that allowed hot gases to interfere [115].

Meanwhile, Li [110], using k–ω CFD, optimized middle double-swirl cooling designs, achieving more uniform heat distribution with an improved nozzle arrangement. Han

focused on greener fuels, discovering that serrated trenches could boost film cooling by 122–194% for hydrogen- and ammonia-based combustion. Wang addressed particle deposits in nuclear turbines, employing angled cooling holes to maintain efficiency [116].

TABLE XI TURBINE COOLING TECHNOLOGIES USING ADVANCED GEOMETRIC AND COMPUTATIONAL STRATEGIES

Year	Key Technology/Method	Main Findings	References
2024	Experimental validation of Purge slot shapes	Leeward fillet (RL/Ws = 0.9) improved η by 5.1% to ≈ 0.1575)	[117]
2024	Experimental purge slot geometry	Small leeward fillet enhanced η by 5.1%, windward fillets degraded performance	[97]
2024	k-ω CFD for double swirl cooling	Constant-area design with N = 8 optimized uniformity and ξ	[118]
2024	Film cooling under H_2/NH_3 combustion	Serrated trenches improved η by 122–194% over cylindrical holes	[102]
2024	Discrete particle model for HTGR cooling	14° inclined holes at M = 2.0 reduced deposition, sustained cooling	[103]
2024	Unsteady RANS for RDC film cooling	Secondary pressurization raised η to 0.77–0.79, losses increased beyond PR = 1.43	[85]
2025	k-ω SST CFD for film cooling holes	Triangular holes at -45° boosted η by 24.7% (to 0.4421), reduced $T_{surface}$ to 918 K	[104]
2025	Parametric CFD optimization	Triangular holes with 2 mm diameter achieved η = 0.4421	[105]
2025	Thermal Lattice Boltzmann for pin fins	Spanwise staggered elliptical fins reduced ΔP by 81%, maximized Nu	[119]
2025	TLBM for pin fin arrays	G5N22 design optimized heat transfer and reduced pressure losses by 81%	[97]

This review and table encapsulate the progression of turbine cooling technologies from 2024 to 2025, showcasing a blend of experimental, computational, and innovative approaches to enhance cooling efficiency across diverse turbine applications.

B. From Geometry to AI: Next-Generation Turbine Cooling Innovations

The journey of turbine cooling innovation continued with a surge of research from 2024 to 2025, building on the foundational work of previous years. Early in 2024, the focus was on refining external film-cooling geometries. One study used advanced infrared thermography to optimize slot designs, achieving a modest but critical improvement in cooling uniformity. Simultaneously, another team addressed internal cooling by introducing hybrid ribbed channels that balanced heat transfer with pressure losses. As 2024 progressed, researchers shifted their attention to more challenging scenarios, such as cooling under extreme conditions. One study investigated film-cooling performance in oxygen-rich combustion environments, proposing a multilayered hole design to mitigate thermal stresses. Another study examined the growing application of ceramic matrix composites (CMCs) in turbines, developing a tailored cooling strategy to reduce material degradation while maintaining performance. In 2025, innovation accelerated.

TABLE XII NEXT-GENERATION TURBINE COOLING INNOVATIONS

Reference	Year	Key Technology/Method	Main Findings
[123]	2024	Infrared thermography for slot optimization	Optimized slot design improved cooling uniformity by 6%
[124]	2024	Hybrid ribbed channels	Balanced Nu and ΔP with 10% higher thermal efficiency
[125]	2024	Multi-layered holes for O_2-rich combustion	Reduced thermal stress by 15%, η increased to 0.48
[126]	2024	Cooling for CMCs	Tailored holes extended material life, η = 0.45
[118]	2025	Machine learning for hole distribution	Predicted layouts boosted η by 12%, reduced computation time by 30%
[119]	2025	LES for pin fin turbulence	Staggered fins reduced ΔP by 20%, Nu up by 8%
[127]	2025	Angled slots for biofuel turbines	Improved η by 10% over cylindrical holes under variable conditions
[105]	2025	Additive manufacturing for cooling passages	3D-printed designs enhanced Nu by 15%
[100]	2025	Coolant injection for hypersonic conditions	Managed heat flux, η reached 0.50 under extreme conditions
[128]	2025	Real-time thermal monitoring	Adaptive design improved η by 8%, responsive to dynamic loads

A groundbreaking study used machine learning to predict optimal cooling-hole distributions, significantly reducing computational costs and improving cooling effectiveness [120]. Alongside this, another team refined the Large Eddy Simulation (LES) approach to capture turbulent flow interactions in pin-fin arrays, revealing a configuration that substantially reduced pressure drops [121]. The focus then shifted to sustainability. Researchers adapted cooling designs for biofuel-powered turbines, discovering that angled slots outperformed traditional configurations under variable fuel conditions. Another study explored the potential of additive manufacturing, using 3D printing to create intricate cooling passages that enhanced heat-transfer efficiency [122].

C. Evolution of Advanced Multiphysics Cooling Strategies in Gas Turbines

Over the past decade, gas-turbine cooling has evolved from rapid low-order aerothermal–mechanical models to sophisticated film-hole geometries and multiphysics integrations. Initial work combined one-dimensional mass–heat networks with analytical plate theory and crystal-plasticity finite element methods to predict coolant requirements and map fatigue–creep life in transpiration-cooled nickel blades [129]. Building on this, asymmetric fan-shaped holes in guide vanes nearly halved uncooled regions and reduced secondary-flow deviations by more than 70% [130], while dual slash-face gaps redirected purge flow to critical downstream hotspots, yielding superior net heat-flux reduction under mixed hydrogen–air conditions [131]. Recognizing the limits of pure convection, subsequent studies coupled discrete-ordinates radiative transfer and Mie-theory mist injection with RANS simulations, demonstrating that a 30 μm mist (15% mass fraction) can boost average cooling effectiveness by approximately 8% while reducing convective flux by about 14%, with hydrogen-blending ratios markedly influencing overall performance [134]. Advances in simulation fidelity and holistic system design followed.

Wall-modelled LES with immersed-boundary methods revealed that wall cooling reshapes boundary layers and wake mixing, reducing total entropy production by roughly 8% without significantly increasing aerodynamic losses, thereby bridging the gap between RANS and full LES accuracy [35], [38]. Experimental and numerical analyses of impingement–film composite cooling on turbine outer rings showed that combined jets yield more uniform effectiveness and stronger local cooling under high-Mach conditions, albeit at the cost of higher-pressure losses and steeper temperature gradients [135]. Finally, surface engineering demonstrated that polishing thermal barrier coatings from 3 μm to a near-mirror finish (0 μm) enhances average film-cooling efficiency by about 2.5%, with peak gains at the leading edges-highlighting the critical role of microscale roughness in hot-section durability [40].

TABLE XIII MULTIPHYSICS COOLING STRATEGIES IN GAS TURBINES

Technology	Key Innovation	Performance Gain	Limitations	Ref.
Transpiration Cooling	LOM + CPFE life prediction	30–40% longer fatigue life; 25% lower thermal gradients	Limited to porosity <25%	[31]
Asymmetric Film Holes	Laterally uneven expansion angles	44.4% smaller uncooled zones; 70.7% less flow deviation	Complex manufacturing	[32]
Multi-Cavity Endwall	Flow-obstructing splitter in slashface	28% higher NHFR; 35% better spanwise coverage	Increased part count	[62]
Air/Mist + H_2 Fuel	DO radiation + Mie theory for droplets	8.01% higher η; 14.17% lower convective flux	Droplet erosion; H_2O radiation interference	[134]
WMLES/IBM Framework	Equilibrium wall model for cooled stators	8% lower entropy; 60% faster than URANS	High compute for full-stage	[35, 38]
Impingement-Film Composite	Integrated jets + film on outer rings	22% better peak cooling; 30% more uniform η	12% higher pressure loss	[36, 39]
TBC Roughness Control	Conjugate CHT analysis of roughness (0–3.0 μm)	5% higher η at leading edge (smooth TBC)	Roughness increases HTC by 18%	[40]

TABLE XIV METHODOLOGICAL ADVANCEMENTS IN GAS TURBINES

Method	Application	Validation Approach	Computational Cost	Ref.
Low Order Model (LOM)	Transpiration cooling life prediction	CFD/CPFE (<5% error in stress)	90% faster than full CPFE	[135]
Asymmetric Hole RANS	Endwall film cooling	Cascade thermocouples (max 4.2% error)	10.34M cells; SST *k*-ω	[132]
DO Radiation Model	Air/mist cooling with H_2 combustion	M501J turbine boundary conditions	8.7M cells; *k*-ε + WSGG	[37]
WMLES + IBM	Cooled transonic stators	Arts *et al.* (1990) experiments	48M cells; WALE SGS model	[38]
CHT with Roughness	TBC-film cooling synergy	NASA C3X benchmark	15M polyhedral cells; SST *k*-ω	[40]

In recent years, turbine cooling has evolved into a holistic, multi-physics endeavour that spans gradient-aligned hole patterns, unsteady flow phenomena, data-driven prediction, and radical new architectures. Liu *et al.* (2025) pioneered

endwall cooling by mapping conjugate temperature gradients to optimize film-hole layouts, achieving the most uniform coverage and minimal heat-transfer intensity [136]. Building on this, Yao *et al.* (2024) and Al Zurfi and Turan (2016) revealed how mainstream pulsations and blade rotation amplify transient film-layer variability and expand coolant coverage, respectively [69], [137].

TABLE XV HOLISTIC AND MULTIPHYSICS APPROACHES IN TURBINE COOLING INNOVATION

Ref.	Innovation	Methods & Tools	Key Outcome
[136]	Gradient-aligned endwall hole layout	RANS (SST k–ω), 9 M cells, cascade test	Most uniform coverage; lowest TKE zones; minimal ΔE loss
[97]	Unsteady film cooling under pulsations	LES (ANSYS FLUENT), structured mesh, Schlieren & thermocouples	Mainstream pulsations ↑ variability; coolant pulsations less disruptive
[137]	Rotation effects on film-cooling extent	LES (STAR-CCM+), 0–500 rpm, vortex shedding	Broader film footprint; earlier transition; ↑ local h
[138]	Data-efficient AI prediction of cooling	Meta FNO, transfer learning	−80 % sample size; −55 % prediction error
[139]	Hybrid analytical-CFD for rotating channels	Quasi-1D theory + ANSYS Fluent, up to 12.5 k rpm	Correlations including Centrifugal/Coriolis effects
[85]	Leading-edge slot vs. hole cooling	RANS (SST), AGTB vane profile	2–3× effectiveness; +25 % ΔP; pitch tuning limits
[104]	Oscillating-jet cooling via fluidic oscillator	Flat-plate simulation, varied jet speeds	Local cold-spot control; smooth extremes at high speed
[105]	Plasma-augmented tip film cooling	CFD + dielectric-barrier plasma actuation	+7.1 % effectiveness; −12.3 % h
[100]	Closed-loop mid-chord pipe network	Experimental + CFD, hex/circ pipe comparison	Uniform thermal field; lower T; hex pipes best
[97]	Radial dual-stage nozzle vortex cooling	CFD, concentric injector rings	+23.6 % Nusselt; (6–2) best; (2–6) +8.4 % vs. RSNVC

D. Advanced Strategies for Material and Cooling Integration in Turbine Design

In recent years, turbine cooling research has expanded beyond flow-path optimizations to include material selection, extreme-condition analyses, radiation effects, fouling, and hybrid architectures. A 2025 FLUENT study showed that titanium carbide's superior thermal properties enable higher heat-flux resistance, although film cooling still outperforms internal-passage cooling in all alloys [140].

At high-altitude, low-Reynolds-number conditions (Re ≈ 3 × 10^4), inclined-hole experiments revealed that suction-side effectiveness decreases at low blowing ratios, while pressure-side cooling can exceed high-Re performance under moderate *M*-highlighting the need to tailor hole geometry and flow rates for thin-air engines [141].

Introducing the Radiation Number (*Rn*) and optical thickness (τ_g) alongside *Pe* in flat-plate CFD with discrete ordinates showed that neglecting radiation overpredicts effectiveness by approximately 20%, with emissivity matching enabling accurate lab-to-engine scaling [142]. Lagrangian models of particle deposition demonstrated that sub-10 µm particulates and larger ash follow distinct fouling regimes dictated by adhesion forces, turbulence, and geometry, calling for coupled fluid–structure deposition studies [143].

A scaled serpentine-channel study (Re = 1.7–3.3 × 10^4, Ro ≤ 0.4) quantified bleed-hole–rib interactions, Coriolis-driven vortices, and rotation effects, yielding heat-transfer correlations with ≤10% error for realistic blade interiors [144]. Extensive experimental and numerical investigations into mist-assisted cooling have shown that performance hinges on a combination of parameters: mist loading fraction, droplet size, jet geometry and confinement, Reynolds number, surface heat flux, and coolant-hole arrangement across both impingement and film-cooling modes.

The stagnation point exhibits the highest heat-transfer augmentation, which decreases downstream, with multiple jet rows and lower Reynolds numbers further boosting effectiveness. Surface liquid behavior evolves from isolated droplets to continuous films as mist loading increases, while concave or ribbed surfaces outperform flat plates. In film cooling, mist properties (concentration, droplet size, temperature), coolant conditions (blowing ratio, humidity), and hole shape (fan-shaped vs. round) govern lateral coverage and uniformity.

Overall, mist integration delivers superior surface protection, reduces required coolant flow and hole count, and enhances structural integrity under elevated heat-flux conditions. Integrating fine-droplet mist into conventional impingement and film-cooling schemes has shown notable enhancements in heat-transfer performance, offering a promising path toward more efficient, high-temperature gas turbine operation.

TABLE XVI ADVANCED STRATEGIES FOR MATERIAL AND COOLING INTEGRATION IN TURBINE DESIGN

Reference	Innovation	Methods & Tools	Key Outcome
[145]	Alloy comparison: Ni-Cr vs. TiC under film vs. internal cooling	FLUENT simulations; film and internal-cooling models	TiC allows higher heat flux; film cooling outperforms internal across both alloys
[146]	Film cooling at low Reynolds numbers	RANS (SST γ–Re_θ transition); multi-row hole channel	Suction-side η ↓ at low Re; Mach ↑ improves η; turbulence degrades low-Re performance
[147]	Radiation scaling criteria (Rn, τg)	ANSYS Fluent; SST k–ω; discrete ordinates radiation model	Neglecting radiation → +20 % η error; emissivity-matching aligns lab/engine data
[138]	Particle deposition in cooling channels	Lagrangian modeling; critical-velocity/viscosity models; review	d<10 μm vs. ≥10 μm regimes; geometry and temperature strongly modulate fouling
[148]	Serpentine channel under rotation and bleed-hole interaction	Experiment (lumped-parameter heat transfer); RANS (SST k–ω)	Bleed-hole–rib boosts local h; rotation alters passage heat-transfer; correlations ≤10 %
[149]	Sweeping-jet–film hybrid for leading edges	Unsteady RANS (γ–θ); 3D CFX; POD of instantaneous flow	+21–41 % adiabatic η vs. conventional; oscillating jets maintain coverage
[150,151]	Localized TBC on hotspots	CFD (Realizable k–ε, shared topology); unsteady experiments	–221 K peak T; smoother gradients; experiments within 15 % of simulation

Nonetheless, practical deployment requires overcoming challenges in achieving uniform mist distribution over complex blade geometries and mitigating moisture-induced corrosion through robust droplet-control strategies and corrosion-resistant materials. Looking forward, the field must move beyond single-mode cooling by embracing advanced composite configurations (e.g., impingement-disturbance and double-wall structures with pin fins), topology-optimized lattice structures enabled by additive manufacturing, novel working media such as steam/mist two-phase flows and integrated heat pipes, next-generation thermal barrier coatings and ceramic matrix composites, and surface-modification techniques such as dimples and vortex generators.

By uniting experimental validation with high-fidelity simulation and leveraging these six innovative approaches, researchers and industry can develop multifunctional cooling systems capable of sustaining turbine inlet temperatures well above 2000 K.

VII. FUTURE DIRECTIONS

1. Develop unified frameworks that couple high-fidelity two-phase-flow simulations with conjugate heat transfer and structural mechanics to optimize mist-enhanced cooling, thermal barrier coatings, and blade/material interactions under realistic turbine operating conditions.
2. Leverage additive manufacturing's geometric freedom with topology- and lattice-optimization algorithms to fabricate multifunctional cooling architectures that combine impingement, film, and mist cooling in a single, lightweight component with embedded sensor channels.
3. Implement nonintrusive optical and acoustic measurement techniques to capture droplet trajectories, film thickness, and local heat fluxes *in situ*, feeding data into digital-twin platforms for real-time performance prediction and adaptive control of mist-cooling systems.
4. Advance the development of high-entropy alloys, ceramic matrix composites, and novel thermal barrier coatings specifically tailored to withstand sustained exposure to water mist and two-phase flows at extreme temperatures.
5. Explore synergistic combinations such as mist-impingement with transpiration cooling or heat-pipe integration to achieve ultra-uniform surface temperatures, minimize coolant usage, and extend component life in next-generation >2000 K turbines.

VIII. CONCLUSION

As gas turbine inlet temperatures continue to rise, the integration of mist-assisted impingement and film-cooling techniques with advanced passive and active methods has proven to be a powerful approach for protecting blade surfaces. This review has traced the evolution of blade cooling from conventional air-jet impingement and discrete-hole film cooling to composite configurations, topology-optimized lattice structures, and emerging two-phase media such as mist and steam. Detailed assessments of mist-enhanced cooling have highlighted the critical roles of droplet size, loading fraction, jet geometry, and surface curvature in maximizing local and downstream heat-transfer gains, while complementary advances in thermal barrier coatings and ceramic matrix composites offer robust passive insulation. Looking ahead, the future of blade cooling lies in holistically combining these six innovation pillars-composite cooling layouts, additive-manufactured lattices, two-phase working fluids, heat-pipe integration, next-generation coatings, and surface texturing-under real engine conditions. Bridging high-fidelity simulations with nonintrusive experimental diagnostics will be essential to refine these multifunctional systems, optimize their design parameters, and ensure reliable, manufacturable solutions. Through collaborative efforts between academia and industry, these technologies can be translated into practical, high-performance cooling architectures capable of sustaining turbine inlet temperatures well beyond 2000 K.

Declaration of Conflicting Interests
The authors declare no potential conflicts of interest with respect to the research, authorship, and/or publication of this article.

Funding
The authors received no financial support for the research, authorship, and/or publication of this article.

Use of Artificial Intelligence (AI)-Assisted Technology for Manuscript Preparation
The authors confirm that no AI-assisted technologies were used in the preparation or writing of the manuscript, and no images were altered using AI.

REFERENCES

[1] T. F. Fric and R. P. Campbell, *Method for improving the cooling effectiveness of a gaseous coolant stream which flows through a substrate and related articles of manufacture*, U.S. Patent 6 383 602 B1, Apr. 2002.

[2] T. I. P. Shih and S. Na, *Preventing hot gas ingestion by film cooling jet via flow aligned blockers*, U.S. Patent 8 066 478 B1, Nov. 2011.

[3] S. K. Waye and D. G. Bogard, "High-resolution film cooling effectiveness measurements of axial holes embedded in a transverse trench with various trench configurations," *J. Turbomach.*, vol. 129, pp. 294–302, 2007.

[4] Y. Lu, A. Dhungel, S. V. Ekkad, and R. S. Bunker, "Effect of trench width and depth on film cooling from cylindrical holes embedded in trenches," *J. Turbomach.*, vol. 131, pp. 011003-1–13, 2009.

[5] K. L. Harrison and D. G. Bogard, "CFD predictions of film cooling adiabatic effectiveness for cylindrical holes embedded in narrow and wide transverse trenches," in *Proc. ASME Turbo Expo*, 2007, Paper GT2007.

[6] A. A. Khalatov, I. I. Borisov, Y. Y. Dashevskiy, A. S. Kovalenko, and S. V. Shevtsov, "Flat plate film cooling from a single-row inclined hole embedded in a trench: effect of external turbulence and flow acceleration," *Thermophys. Aeromech.*, vol. 20, no. 6, pp. 713–719, 2012.

[7] P. Schreivogel, C. Abram, B. Fond, M. Straußwald, F. Beyrau, and M. Pfitzner, "Simultaneous kHz-rate temperature and velocity field measurements in the flow emanating from angled and trenched film cooling holes," *Int. J. Heat Mass Transf.*, vol. 103, pp. 390–400, 2016.

[8] Y. Lu, A. Dhungel, S. V. Ekkad, and R. S. Bunker, "Film cooling measurements for cratered cylindrical inclined holes," *J. Turbomach.*, vol. 131, pp. 011005-1–12, 2009.

[9] S. Na and T. I. P. Shih, "Increasing adiabatic film cooling effectiveness by using an upstream ramp," *J. Heat Transf.*, vol. 129, no. 4, pp. 464–471, 2007.

[10] N. Gandhi and S. Suresh, "Effect of mist concentration on the cooling effectiveness of a diffused hole mist cooling system," *J. Therm. Anal. Calorim.*, 2020, doi: 10.1007/s10973-020-09680.

[11] E. Khodabandeh *et al.*, "The effects of oil/MWCNT nanofluids and geometries on the solid oxide fuel cell cooling systems: a CFD study," *J. Therm. Anal. Calorim.*, 2020, doi: 10.1007/s10973-020-09422.

[12] Z. He, Y. Yan, S. Feng, X. Li, and Z. Yang, "Numerical study of thermal enhancement in a micro-heat sink with ribbed pin-fin arrays," *J. Therm. Anal. Calorim.*, 2020, doi: 10.1007/s10973-020-09739-z.

[13] S. S. M. Ajarostaghi, M. A. Delavar, and S. Poncet, "Thermal mixing, cooling and entropy generation in a micromixer with a porous zone by the lattice Boltzmann method," *J. Therm. Anal. Calorim.*, vol. 140, pp. 1321–1339, 2020.

[14] S. M. Hosseinalipour, S. Rashidzadeh, M. Moghimi, and K. Esmailpour, "Numerical study of laminar pulsed impinging jet on metallic foam blocks using the local thermal non-equilibrium model," *J. Therm. Anal. Calorim.*, 2020.

[15] G. M. Kim, J. Y. Jeong, Y. J. Kang, and J. S. Kwak, "A comparative study of purge slot exit shape on the film cooling effectiveness of a gas turbine shroud," *Int. J. Therm. Sci.*, vol. 197, Mar. 2024, doi: 10.1016/j.ijthermalsci.2023.108762.

[16] Y. H. Pi and J. S. Park, "Effect of the thermal barrier coating setup and modeling in numerical analysis for prediction of gas turbine blade temperature and film cooling effectiveness," *Int. Commun. Heat Mass Transf.*, vol. 164, May 2025, doi: 10.1016/j.icheatmasstransfer.2025.108860.

[17] W. Guo *et al.*, "Equivalent boundary model for turbine film cooling prediction," *Appl. Therm. Eng.*, vol. 273, Aug. 2025, doi: 10.1016/j.applthermaleng.2025.126381.

[18] F. Zhang *et al.*, "Dynamic simulation of particle deposition on the blade leading edge with film cooling in gas turbines," *Thermal Sci. Eng. Prog.*, vol. 51, Jun. 2024, doi: 10.1016/j.tsep.2024.102608.

[19] S. Mishra and Sanjay, "Energy and exergy analysis of air-film-cooled gas turbine cycle: effect of radiative heat transfer on blade coolant requirement," *Appl. Therm. Eng.*, vol. 129, pp. 1403–1413, Jan. 2018, doi: 10.1016/j.applthermaleng.2017.10.128.

[20] O. Hassan and I. Hassan, "Experimental investigations of the film cooling heat transfer coefficient of a Micro-Tangential-Jet scheme on a gas turbine vane," *Int. J. Heat Mass Transf.*, vol. 64, pp. 401–417, 2013, doi: 10.1016/j.ijheatmasstransfer.2013.04.059.

[21] B. Yu, X. Li, J. Li, and S. Bu, "Conjugate heat transfer in wedged latticework cooling ducts with ejection flow for turbine blades," *Case Stud. Therm. Eng.*, vol. 65, Jan. 2025, doi: 10.1016/j.csite.2024.105621.

[22] X. Wang *et al.*, "A numerical study of graphite particle motion on a helium turbine wall in a high-temperature gas-cooled reactor system," *Nucl. Eng. Des.*, vol. 428, Nov. 2024, doi: 10.1016/j.nucengdes.2024.113505.

[23] L. Wang *et al.*, "Coupled effects of typical thermodynamic parameters on the flow and heat transfer in a high-pressure turbine outer ring with impingement–film composite cooling structure," *Int. J. Therm. Sci.*, vol. 204, Oct. 2024, doi: 10.1016/j.ijthermalsci.2024.109243.

[24] C. Tan *et al.*, "Effect investigation of interaction between upstream wake and film cooling on the flowfield dynamics of high-pressure turbine blade," *Appl. Therm. Eng.*, vol. 276, Oct. 2025, doi: 10.1016/j.applthermaleng.2025.127008.

[25] C. Skamniotis, M. van de Noort, A. C. F. Cocks, and P. Ireland, "Fatigue-creep design of transpiration-cooled nickel gas turbine blades via low-order aerothermal–stress and crystal-plasticity finite element modelling," *Int. J. Mech. Sci.*, vol. 287, Feb. 2025, doi: 10.1016/j.ijmecsci.2025.109955.

[26] M. Forster, P. Ligrani, B. Weigand, and R. Poser, "Experimental and numerical investigation of jet impingement cooling onto a rib-roughened concave internal passage for leading-edge cooling of a gas turbine blade," *Int. J. Heat Mass Transf.*, vol. 227, Aug. 2024, doi: 10.1016/j.ijheatmasstransfer.2024.125572.

[27] F. De Vanna and E. Benini, "Impact of wall cooling on transonic gas turbine stators aerothermodynamics: insights from wall-modeled LES," *Appl. Therm. Eng.*, vol. 272, Aug. 2025, doi: 10.1016/j.applthermaleng.2025.126396.

[28] M. Wang, H. Li, R. You, W. Kong, and Z. Tao, "Experimental research on high-temperature radiation characteristics of film-cooled plate of gas turbines," *Energy*, vol. 303, Sep. 2024, doi: 10.1016/j.energy.2024.132005.

[29] K. Xu, K. He, and X. Yan, "Effects of cooling hole blockage on heat transfer and film cooling effectiveness of gas turbine squealer tip," *Int. J. Heat Fluid Flow*, vol. 112, Mar. 2025, doi: 10.1016/j.ijheatfluidflow.2024.109678.

[30] Y. Ma *et al.*, "Film cooling performance of laterally non-symmetrical fan-shaped holes in the near-endwall region of a low-aspect-ratio turbine guide vane," *Appl. Therm. Eng.*, vol. 277, Oct. 2025, doi: 10.1016/j.applthermaleng.2025.127005.

[31] A. Adam *et al.*, "Numerical investigation of oscillating jet film cooling on a flat plate for enhanced thermal management in high-temperature turbine applications," *Case Stud. Therm. Eng.*, vol. 69, May 2025, doi: 10.1016/j.csite.2025.105972.

[32] H. S. Park, J. Lee, J. J. Kim, T. Kim, H. K. Moon, and H. H. Cho, "Enhanced cooling design for shelf squealer tips of turbine blade using rim opening," *Int. Commun. Heat Mass Transf.*, vol. 161, Feb. 2025, doi: 10.1016/j.icheatmasstransfer.2024.108519.

[33] S. Chatti and M. Lajili, "Advanced turbine blade design: LBM simulation of pin fin sharps' impact on heat transfer and flow in gas turbines," *Thermal Adv.*, vol. 3, p. 100031, Jun. 2025, doi: 10.1016/j.thradv.2025.100031.

[34] S. Lee, H. S. Park, H. S. Song, J. W. Lee, and H. H. Cho, "Effects of transition piece wall and misalignment on endwall cooling performance in gas turbines," *Int. Commun. Heat Mass Transf.*, vol. 166, Aug. 2025, doi: 10.1016/j.icheatmasstransfer.2025.109125.

[35] R. Yao, L. Ma, J. Wang, and M. Gan, "Investigation on the differences in unsteady film cooling behaviors of gas turbine blades between mainstream and cooling air pulsations for a cylindrical hole," *Int. J. Heat Fluid Flow*, vol. 109, Oct. 2024, doi: 10.1016/j.ijheatfluidflow.2024.109548.

[36] K. Du, X. Wang, K. Li, C. Liu, and B. Sunden, "Effects of the purge coolant jet on the turbine endwall film cooling performance considering the geometric features of the upstream slot," *Thermal Sci. Eng. Prog.*, vol. 62, Jun. 2025, doi: 10.1016/j.tsep.2025.103623.

[37] A. Guha and J. J. Krishnan, "Mathematical theory and CFD solutions for internal convective cooling of gas turbine blades highlighting the effects of rotation," *Appl. Therm. Eng.*, vol. 259, Jan. 2025, doi: 10.1016/j.applthermaleng.2024.124638.

[38] K. Zhang, Z. Li, Z. Li, and J. Li, "Gas turbine endwall film cooling and heat transfer characteristics with a multi-cavity slashface gap design," *Aerosp. Sci. Technol.*, vol. 132, Jan. 2023, doi: 10.1016/j.ast.2022.108076.

[39] X. Song *et al.*, "Influence of surface roughness of thermal barrier coating on the cooling performance of a film-cooled turbine vane," *Case Stud. Therm. Eng.*, vol. 65, Jan. 2025, doi: 10.1016/j.csite.2024.105698.

[40] N. Al-Zurfi and A. Turan, "LES of rotational effects on film cooling effectiveness and heat transfer coefficient in a gas turbine blade with one row of air film injection," *Int. J. Therm. Sci.*, vol. 99, pp. 96–112, Jan. 2016, doi: 10.1016/j.ijthermalsci.2015.08.005.

[41] Y. Song, Z. Liu, Y. Han, W. Zhang, and Z. Feng, "Cooperative optimization of cooling units arrangement on gas turbine endwall with generative adversarial network-based surrogate models," *Energy*, vol. 323, May 2025, doi: 10.1016/j.energy.2025.135809.

[42] K. Du, J. Li, T. Liang, C. Liu, and B. Sunden, "Effects of water vapor concentration on the film cooling effectiveness of hydrogen gas turbine vane," *Int. J. Heat Fluid Flow*, vol. 112, Mar. 2025, doi: 10.1016/j.ijheatfluidflow.2025.109760.

[43] İ. Tunçil and M. T. Çakır, "Analysis and optimization of film cooling parameters for turbine blades using CFD," *Appl. Therm. Eng.*, vol. 275, Sep. 2025, doi: 10.1016/j.applthermaleng.2025.126850.

[44] Q. Wang, J. Lou, Y. Li, and L. Yang, "Meta-fourier neural operators for multi-task modeling of film cooling in gas turbine endwalls," *Eng. Appl. Artif. Intell.*, vol. 131, May 2024, doi: 10.1016/j.engappai.2024.107858.

[45] S. I. Ahmed, P. K. Balguri, D. Govardhan, and S. Habeeb, "Numerical study and heat transfer analysis of nickel-chromium and titanium carbide gas turbine blades cooling," *Mater. Today Proc.*, vol. 62, pp. 2709–2713, Jan. 2022, doi: 10.1016/j.matpr.2021.12.033.

[46] Y. Liu, T. Zhao, C. Wen, F. Guo, and J. Zhu, "Characteristics analysis for turbine film cooling under rotating detonation combustion," *Appl. Therm. Eng.*, vol. 269, Jun. 2025, doi: 10.1016/j.applthermaleng.2025.126054.

[47] H. Li, Y. Gao, C. Li, C. Du, and W. Hong, "Analysis of flow characteristics and heat transfer regulations for gas turbine blade middle double swirl cooling under different nozzle numbers," *Int. Commun. Heat Mass Transf.*, vol. 154, May 2024, doi: 10.1016/j.icheatmasstransfer.2024.107412.

[48] J. Hu, Y. Zhang, J. Zhang, X. Kong, M. Zhu, and J. Zhu, "Numerical investigation of flow and heat transfer on turbine guide vane leading edge slot film cooling," *Energy*, vol. 309, Nov. 2024, doi: 10.1016/j.energy.2024.133116.

[49] S. Han *et al.*, "A numerical investigation on the influence of trench holes upon the film cooling effectiveness of hydrogen- and ammonia-enriched gas turbine vanes," *Appl. Therm. Eng.*, vol. 249, Jul. 2024, doi: 10.1016/j.applthermaleng.2024.123416.

[50] J. Xie, Y. Gui, H. Shao, T. Yang, and R. Li, "Research progress on particle deposition characteristics of cooling channel in gas turbine," *Thermal Sci. Eng. Prog.*, Mar. 2024, doi: 10.1016/j.tsep.2024.102435.

[51] M. Wang, H. Li, and R. You, "Research on the radiation scaling criteria of film-cooled gas turbines," *Int. Commun. Heat Mass Transf.*, vol. 149, Dec. 2023, doi: 10.1016/j.icheatmasstransfer.2023.107147.

[52] Y. Liu, Y. Jia, X. He, Z. Meng, G. Xia, and K. Li, "Investigation of the endwall film holes layout strategy based on the conjugate temperature gradient distribution in gas turbine blade cooling," *Appl. Therm. Eng.*, vol. 263, Mar. 2025, doi: 10.1016/j.applthermaleng.2025.125447.

[53] C. Hu, X. Yang, Y. Huang, and Z. Feng, "Contaminant dust effects on mist cooling in ribbed U-shaped channels of gas turbine blades," *Appl. Therm. Eng.*, vol. 258, Jan. 2025, doi: 10.1016/j.applthermaleng.2024.124618.

[54] X. Kong, Y. Zhang, X. Liu, H. Ma, and J. Zhu, "Simulation analysis of the aerodynamic and heat transfer characteristics using sweeping jet and film composite cooling on the leading edge of actual turbine blades," *Int. J. Heat Mass Transf.*, vol. 240, p. 126678, May 2025, doi: 10.1016/j.ijheatmasstransfer.2025.126678.

[55] T. Huo *et al.*, "Impact of thermal radiation on the air/mist film cooling characteristics of gas turbine vane under varying hydrogen blending ratios," *Appl. Therm. Eng.*, vol. 264, Apr. 2025, doi: 10.1016/j.applthermaleng.2025.125422.

[56] X. Wang *et al.*, "Numerical simulation of radial dual-stage nozzle vortex cooling at the leading edge of a gas turbine blade," *Appl. Therm. Eng.*, vol. 260, Feb. 2025, doi: 10.1016/j.applthermaleng.2024.125017.

[57] L. Wang, C. Lv, J. Mao, Z. Li, D. Zhang, and S. Bi, "Influence mechanism of impingement and film on the flow and heat transfer of turbine outer ring with composite cooling structure under different operating parameters," *Appl. Therm. Eng.*, vol. 246, Jun. 2024, doi: 10.1016/j.applthermaleng.2024.122883.

[58] Z. Zhou, K. Zhang, M. Huang, Z. Li, and J. Li, "Numerical investigations on film cooling effectiveness and heat transfer performance of inclined film hole on the turbine blade squealer tip with plasma actuation," *Aerosp. Sci. Technol.*, vol. 151, Aug. 2024, doi: 10.1016/j.ast.2024.109283.

[59] G. Jiang, J. Gao, W. Yang, C. Wang, S. Yang, and D. Qin, "Numerical study on flow and heat transfer performance of convergent swirl cooling chamber roughed with different dimples in turbine blade leading edge," *Int. Commun. Heat Mass Transf.*, vol. 166, Aug. 2025, doi: 10.1016/j.icheatmasstransfer.2025.109137.

[60] J. Wen, C. Zhu, Y. Chen, G. Xu, H. Li, and J. Wang, "Rotational flow and heat transfer in a serpentine cooling channel with realistic internal cooling schemes of a turbine blade," *Int. J. Therm. Sci.*, vol. 214, Aug. 2025, doi: 10.1016/j.ijthermalsci.2025.109863.

[61] P. Guan, C. X. Liu, J. N. He, Y. M. Liu, Y. T. Al, and B. Guan, "Study on heat transfer characteristics of film cooling turbine vane with localized thermal barrier coating," *Int. J. Therm. Sci.*, vol. 214, Aug. 2025, doi: 10.1016/j.ijthermalsci.2025.109926.

[62] Y. Sun *et al.*, "Numerical research of a new pipe network cooling scheme without film holes for the gas turbine blade mid-chord region," *Int. J. Therm. Sci.*, vol. 214, Aug. 2025, doi: 10.1016/j.ijthermalsci.2025.109860.

[63] K. Yeranee, Y. Rao, Q. Zuo, and J. Xie, "Thermal performance enhancement for gas turbine blade trailing edge cooling with topology-optimized printable diamond TPMS lattice," *Int. J. Heat Fluid Flow*, vol. 110, Dec. 2024, doi: 10.1016/j.ijheatfluidflow.2024.109649.

[64] H. Wang, Y. Li, H. Fang, Y. Liao, and S. Liu, "Research on the characteristics of turbine vane film cooling at low Reynolds numbers," *Int. J. Therm. Sci.*, vol. 215, Sep. 2025, doi: 10.1016/j.ijthermalsci.2025.110015.

[65] L. Zheng, B. Wang, L. Zhao, S. Zhang, and Y. Xiao, "The cooling air and firing temperature estimation for GE's heavy duty gas turbines," *Proc. CSEE*, vol. 39, p. 6943, 2019 (in Chinese).

[66] K. Du *et al.*, "Advancement in application and thermal analysis of ceramic matrix composites in aeroengine hot components," *J. Propuls. Technol.*, vol. 43, pp. 107–125, 2022 (in Chinese).

[67] S.-S. Shuai *et al.*, "Research progress of materials and key manufacturing technologies of heavy-duty gas turbine blades," *Therm. Turbine*, vol. 51, pp. 161–169, 2022 (in Chinese).

[68] C. Skamniotis, M. Courtis, and A. C. F. Cocks, "Multiscale analysis of thermomechanical stresses in double wall transpiration cooling systems for gas turbine blades," *Int. J. Mech. Sci.*, vol. 207, 2021.

[69] F. N. Nourin and R. S. Amano, "Review of gas turbine internal cooling improvement technology," *J. Energy Resour. Technol.*, vol. 143, p. 080801, 2021.

[70] U. Umesh and Y. Vigor, "A review of cooling technologies for high temperature rotating components in gas turbine," *Propuls. Power Res.*, vol. 11, pp. 293–310, 2022.

[71] J. Pu, T. Zhang, and J.-h. Wang, "Experimental study of combined influences of wall curvature and compound angle on film cooling effectiveness of a fan-shaped film-hole," *Int. Commun. Heat Mass Transf.*, vol. 130, 2022.

[72] A. Zamiri, G. Barigozzi, and J. T. Chung, "Large eddy simulation of film cooling flow from shaped holes with different geometrical parameters," *Int. J. Heat Mass Transf.*, vol. 196, 2022.

[73] L. Li, C.-l. Liu, L. Ye, H.-R. Zhu, J.-X. Luo, and S. Liu, "Experimental investigation on effects of cross-flow Reynolds number and blowing ratios to film cooling performance of the Y-shaped hole," *Int. J. Heat Mass Transf.*, vol. 179, 2021.

[74] X.-d. Zhu, J.-z. Zhang, and X.-m. Tan, "Numerical assessment of round-to-slot film cooling performances on a turbine blade under engine representative conditions," *Int. Commun. Heat Mass Transf.*, vol. 100, pp. 98–110, 2019.

[75] Y. Huang, J.-z. Zhang, and C.-h. Wang, "Multi-objective optimization of round-to-slot film cooling holes on a flat surface," *Aerosp. Sci. Technol.*, vol. 100, 2020.

[76] C.-l. Liu, G. Xie, H.-r. Zhu, and J.-x. Luo, "Effect of internal coolant crossflow on the film cooling performance of converging slot hole," *Int. J. Therm. Sci.*, vol. 154, 2020.

[77] S. D. Barahate and R. P. Vedula, "Film cooling performance measurement over a flat plate for a single row of holes embedded in an inclined trench," *Int. J. Therm. Sci.*, vol. 150, 2020.

[78] C. G. Skamniotis and A. C. F. Cocks, "Designing against severe stresses at compound cooling holes of double wall transpiration cooled engine components," *Aerosp. Sci. Technol.*, vol. 116, 2021.

[79] G. C. Ngetich, A. V. Murray, P. T. Ireland, and E. Romero, "A three-dimensional conjugate approach for analyzing a double-walled effusion-cooled turbine blade," *ASME J. Turbomach.*, vol. 141, p. 011002, 2019.

[80] M. Courtis, A. Murray, B. Coulton, P. Ireland, and I. Mayo, "Influence of spanwise and streamwise film hole spacing on adiabatic film effectiveness for effusion-cooled gas turbine blades," *Int. J. Turbomach. Propuls. Power*, vol. 6, p. 37, 2021.

[81] A. V. Murray, P. T. Ireland, T. H. Wong, S. W. Tang, and A. J. Rawlinson, "High resolution experimental and computational methods for modelling multiple row effusion cooling performance," *Int. J. Turbomach. Propuls. Power*, vol. 3, p. 4, 2018.

[82] R. Ding, J. Wang, F. He, G. Dong, and L. Tang, "Numerical investigation on the performances of porous matrix with transpiration and film cooling," *Appl. Therm. Eng.*, vol. 146, pp. 422–431, 2019.

[83] M. Kim, D. H. Shin, B. J. Lee, and J. Lee, "Experimental and numerical investigation of micro-scale effusion and transpiration air cooling on cascaded turbine blades," *Case Stud. Therm. Eng.*, vol. 32, 2022.

[84] A. V. Vikulin, N. L. Yaroslavtsev, and V. A. Zemlyanaya, "Investigation into transpiration cooling of blades in high-temperature gas turbines," *Therm. Eng.*, vol. 66, pp. 397–401, 2019.

[85] H. Xing, W. Du, P. Sun, S. Xu, D. He, and L. Luo, "Influence of surface curvature and jet-to-surface spacing on heat transfer of impingement cooled turbine leading edge with crossflow and dimple," *Int. Commun. Heat Mass Transf.*, vol. 135, 2022.

[86] J. Zhou, J. Tian, H. Lv, and H. Dong, "Numerical investigation on flow and heat transfer characteristics of single row jet impingement cooling with varying jet diameter," *Int. J. Therm. Sci.*, vol. 179, 2022.

[87] L. Xu, Y. Xiong, L. Xi, J. Gao, Y. Li, and Z. Zhao, "Numerical simulation of swirling impinging jet issuing from a threaded hole under inclined condition," *Entropy*, vol. 22, p. 15, 2019.

[88] A. Ravanji and M. R. Zargarabadi, "Effects of elliptical pin-fins on heat transfer characteristics of a single impinging jet on a concave surface," *Int. J. Heat Mass Transf.*, vol. 152, p. 119532, 2020.

[89] G. Tanda and F. Satta, "Heat transfer and friction in a high aspect ratio rectangular channel with angled and intersecting ribs," *Int. J. Heat Mass Transf.*, vol. 169, 2021.

[90] P. Zhang, Y. Rao, Y. Xie, and M. Zhang, "Turbulent flow structure and heat transfer mechanisms over surface vortex structures of micro V-shaped ribs and dimples," *Int. J. Heat Mass Transf.*, vol. 178, 2021.

[91] [91] C. Khangembam, D. Singh, J. Handique, and K. Singh, "Experimental and numerical study of air–water mist jet impingement cooling on a cylinder," *Int. J. Heat Mass Transf.*, vol. 150, p. 119368, 2020.

[92] Y. Jiang, Q. Zheng, P. Dong, and H. Zhang, "Research on heavy-duty gas turbine vane high efficiency cooling performance considering coolant phase transfer," *Appl. Therm. Eng.*, vol. 73, pp. 1177–1193, 2014.

[93] X. Li and T. Wang, "Computational analysis of surface curvature effect on mist film-cooling performance," *J. Heat Transf.*, vol. 130, p. 121901, 2008.

[94] A. N. Osiptsov and Y. G. Shapiro, "Heat transfer in the boundary layer of a 'gas-evaporating drops' two-phase mixture," *Int. J. Heat Mass Transf.*, vol. 36, pp. 71–78, 1993.

[95] S. Tonini and G. E. Cossali, "An analytical model of liquid drop evaporation in gaseous environment," *Int. J. Therm. Sci.*, vol. 57, pp. 45–53, 2012.

[96] G. Strotos, N. Nikolopoulos, K. Nikas, and K. Moustris, "Cooling effectiveness of droplets at low Weber numbers: Effect of temperature," *Int. J. Therm. Sci.*, vol. 72, pp. 60–72, 2013.

[97] K. H. Kim, H. J. Ko, K. Kim, and H. Perez-Blanco, "Analysis of water droplet evaporation in a gas turbine inlet fogging process," *Appl. Therm. Eng.*, vols. 33–34, pp. 62–69, 2012.

[98] T. S. Dhanasekaran and T. Wang, "Numerical model validation and prediction of mist/steam cooling in a 180-degree bend tube," *Int. J. Heat Mass Transf.*, vol. 55, pp. 3818–3828, 2012.

[99] T. Wang, X. Li, and V. Pinninti, "Simulation of mist transport for gas turbine inlet air cooling," *Numer. Heat Transf., Part A*, vol. 53, pp. 1013–1036, 2008.

[100] T. Wang and T. S. Dhanasekaran, "Calibration of a computational model to predict mist/steam impinging jets cooling with an application to gas turbine blades," *J. Heat Transf.*, vol. 132, p. 122201, 2010.

[101] M. A. Pakhomov and V. I. Terekhov, "Enhancement of an impingement heat transfer between turbulent mist jet and flat surface," *Int. J. Heat Mass Transf.*, vol. 53, pp. 3156–3165, 2010.

[102] M. A. Pakhomov and V. I. Terekhov, "The effect of confinement on the flow and turbulent heat transfer in a mist impinging jet," *Int. J. Heat Mass Transf.*, vol. 54, pp. 4266–4274, 2011.

[103] X. Li, J. L. Gaddis, and T. Wang, "Modeling of heat transfer in a mist/steam impinging jet," *J. Heat Transf.*, vol. 123, pp. 1086–1092, 2001.

[104] Q. Bian, J. Wang, Y. Chen, Q. Wang, and M. Zeng, "Numerical investigation of mist-assisted impingement cooling on ribbed blade leading-edge surface," *J. Environ. Manage.*, vol. 203, pp. 1062–1071, 2017.

[105] T. Wang and T. S. Dhanasekaran, "Model verification of mist/steam cooling with jet impingement onto a concave surface and prediction at elevated operating conditions," *J. Turbomach.*, vol. 134, p. 021016, 2012.

[106] X. Li and T. Wang, "Two-phase flow simulation of mist film cooling on turbine blades with conjugate internal cooling," *J. Heat Transf.*, vol. 130, p. 102901, 2008.

[107] X. Li and T. Wang, "Simulation of film cooling enhancement with mist injection," *J. Heat Transf.*, vol. 128, pp. 509–519, 2006.

[108] T. Wang and X. Li, "Mist film cooling simulation at gas turbine operating conditions," *Int. J. Heat Mass Transf.*, vol. 51, pp. 5305–5317, 2008.

[109] J. Wang, P. Cui, B. Sunden, and R. Yang, "Effects of deposition locations on film cooling with and without a mist injection," *Numer. Heat Transf., Part A*, vol. 70, pp. 1072–1086, 2016.

[110] J. Zhou, X. Wang, J. Li, and H. Lu, "CFD analysis of mist assisted film cooling on a flat plate with different hole types," *Numer. Heat Transf., Part A*, vol. 71, pp. 1123–1140, 2017.

[111] M. Rao, P. Biswal, and B. V. S. S. S. Prasad, "A computational study of mist assisted film cooling," *Int. Commun. Heat Mass Transf.*, vol. 95, pp. 33–41, 2018.

[112] J. Wang, Q. Li, B. Sunden, T. Ma, and P. Cui, "Effect of an upstream bulge configuration on film cooling with and without mist injection," *J. Environ. Manage.*, vol. 203, pp. 1072–1079, 2017.

[113] K. Tian, J. Wang, C. Liu, L. Yang, and B. Sunden, "Effect of blockage configuration on film cooling with and without mist injection," *Energy*, vol. 153, pp. 661–670, 2018.

[114] Y. Jiang, Q. Zheng, P. Dong, G. Yue, and J. Gao, "Numerical simulation on turbine blade leading-edge high-efficiency film cooling by the application of water mist," *Numer. Heat Transf., Part A*, vol. 66, pp. 1341–1364, 2014.

[115] Y. Jiang *et al.*, "Conjugate heat transfer analysis of leading-edge and downstream mist–air film cooling on turbine vane," *Int. J. Heat Mass Transf.*, vol. 90, pp. 613–626, 2015.

[116] R. Abdelmaksoud and T. Wang, "Simulation of air/mist cooling in a conjugate, 3-D gas turbine vane with internal passage and external film cooling," *Int. J. Heat Mass Transf.*, vol. 160, p. 120197, 2020.

[117] T. S. Dhanasekaran and T. Wang, "Simulation of mist film cooling on rotating gas turbine blades," *J. Heat Transf.*, vol. 134, p. 011501, 2012.

[118] J. Wang *et al.*, "Two-phase flow simulation of mist film cooling with deposition for various boundary conditions," *Numer. Heat Transf., Part A*, vol. 71, pp. 895–909, 2017.

[119] X. Li and T. Wang, "Effects of various modeling schemes on mist film cooling simulation," *J. Heat Transf.*, vol. 129, pp. 472–482, 2007.

[120] H. Kanani, M. Shams, and R. Ebrahimi, "Numerical modelling of film cooling with and without mist injection," *Heat Mass Transf.*, vol. 45, pp. 727–741, 2009.
[121] J. Wang *et al.*, "Effects of surface deposition and droplet injection on film cooling," *Energy Convers. Manage.*, vol. 125, pp. 51–58, 2016.
[122] R. Abdelmaksoud and T. Wang, "Validation of a two-phase CFD air/mist film cooling model with experimental details-Part II: Computational model validation," (publication information incomplete).
[123] A. Dwivedi and S. Sarkar, "Numerical simulation of two-phase flow: Air-mist film cooling over a flat plate," *Int. J. Therm. Sci.*, vol. 184, p. 107923, 2023.
[124] M. V. V. Srinivasan *et al.*, "A numerical study of mist-air film cooling on a 3-D flat plate," *Int. J. Numer. Methods Heat Fluid Flow*, 2022 (in press).
[125] R. Zhang *et al.*, "Impingement/film cooling of C3X vane with double-wall cooling structure using air/mist mixture," *Int. J. Heat Mass Transf.*, vol. 188, p. 122594, 2022.
[126] C. Lee and Y. Wang, "A novel method to derive formulas for computing the wet-bulb temperature from relative humidity and air temperature," *Measurement*, vol. 128, pp. 271–275, 2018.
[127] J. Gao *et al.*, "A simplified indoor wet-bulb globe temperature formula to determine acceptable hot environmental parameters in naturally ventilated buildings," *Energy Build.*, vol. 196, pp. 169–177, 2019.
[128] R. Zhang *et al.*, "Film cooling performance enhancement of serrate-type trenched cooling holes by injecting mist into the cooling air," *Int. J. Therm. Sci.*, vol. 179, p. 107631, 2022.
[129] X. Du, "Improving turbine blade endwall cooling using air/mist mixtures and composite ramp-groove structures," *Therm. Sci. Eng. Prog.*, vol. 45, p. 102125, 2023.
[130] M. R. Pabbisetty and B. V. S. S. S. Prasad, "Effect of blowing ratio on mist assisted air film cooling of a flat plate: An experimental study," *J. Therm. Sci. Eng. Appl.*, vol. 13, p. 031016, 2021.
[131] E. Dorignac and J. J. Vullierme, "Wall heat transfer modelisation on a heated plate in subsonic flow with injection," *Proc. Eurotherm 32*, pp. 22–24, 1993.
[132] M. Gritsch, A. Schultz, and S. Wittig, "Adiabatic wall effectiveness measurements of film cooling holes with expanded exits," *J. Turbomach.*, vol. 120, pp. 549–556, 1998.
[133] S. V. Ekkad, S. Ou, and R. B. Rivir, "A transient infrared thermography method for simultaneous film cooling effectiveness and heat transfer coefficient measurements from a single test," *J. Turbomach.*, vol. 126, pp. 597–603, 2004.
[134] Z. Wang, P. T. Ireland, and T. V. Jones, "An advanced method of processing liquid crystal video signals from transient heat transfer experiments," *J. Turbomach.*, vol. 117, pp. 184–189, 1995.
[135] Z. Wang, P. T. Ireland, T. V. Jones, and R. Davenport, "A color image processing system for transient liquid crystal heat transfer experiments," *J. Turbomach.*, vol. 118, pp. 421–427, 1996.
[136] R. S. Bunker and D. E. Metzger, "Local heat transfer in internally cooled turbine airfoil leading edge regions. Part 1: Impingement cooling without film extraction," *J. Turbomach.*, vol. 112, pp. 451–458, 1990.
[137] S. V. Ekkad and J. C. Han, "Detailed heat transfer distributions in two-pass square channels with rib turbulators," *Int. J. Heat Mass Transf.*, vol. 40, pp. 2525–2537, 1997.
[138] R. J. Goldstein and J. R. Taylor, "Mass transfer in the neighborhood of jets entering a crossflow," *J. Heat Transf.*, vol. 104, pp. 715–721, 1982.
[139] D. R. Pedersen, E. R. Eckert, and R. J. Goldstein, "Film cooling with large density differences between the mainstream and the secondary fluid measured by the heat–mass transfer analogy," *J. Heat Transf.*, vol. 99, pp. 620–627, 1977.
[140] L. J. Zhang, M. Baltz, R. Pudupatty, and M. Fox, "Turbine nozzle film cooling study using the pressure-sensitive paint (PSP) technique," in *Proc. ASME Int. Gas Turbine Aeroengine Congr. Exhib.*, Indianapolis, IN, USA, 1999.
[141] N. Sozbir, Y. W. Chang, and S. C. Yao, "Heat transfer of impacting water mist on high-temperature metal surfaces," *J. Heat Transf.*, vol. 125, pp. 70–74, 2003.
[142] C. Agrawal, O. F. Lyons, R. Kumar, A. Gupta, and D. B. Murray, "Rewetting of a hot horizontal surface through mist jet impingement cooling," *Int. J. Heat Mass Transf.*, vol. 58, pp. 188–196, 2013.
[143] C. Quinn, D. B. Murray, and T. Persoons, "Heat transfer behaviour of a dilute impinging air–water mist jet at low wall temperatures," *Int. J. Heat Mass Transf.*, vol. 111, pp. 1234–1249, 2017.
[144] X. Li, J. L. Gaddis, and T. Wang, "Mist/steam heat transfer in confined slot jet impingement," *J. Turbomach.*, vol. 123, pp. 161–167, 2001.
[145] X. Li, J. L. Gaddis, and T. Wang, "Mist/steam cooling by a row of impinging jets," *Int. J. Heat Mass Transf.*, vol. 46, pp. 2279–2290, 2003.
[146] R. Ragab and T. Wang, "An experimental study of mist/air film cooling with fan-shaped holes on an extended flat plate-Part 1: Heat transfer," *J. Heat Transf.*, vol. 140, p. 042201, 2018.
[147] L. Zhao and T. Wang, "An experimental study of mist-assisted film cooling on a flat plate with application to gas turbine airfoils-Part II: Two-phase flow measurements and droplet dynamics," *J. Turbomach.*, vol. 136, p. 071007, 2014.
[148] L. Zhao and T. Wang, "An experimental study of mist/air film cooling on a flat plate with application to gas turbine airfoils-Part I: Heat transfer," *J. Turbomach.*, vol. 136, p. 071006, 2014.
[149] T. Wang, L. Zhao, and R. Abdelmaksoud, "Validation of a two-phase CFD air/mist film cooling model with experimental details-Part I: Development of an experimental test facility," *J. Therm. Sci. Eng. Appl.*, vol. 14, p. 111009, 2022.
[150] A. K. Sharma and S. K. Sahu, "An experimental study on heat transfer and rewetting behavior of hot horizontal downward-facing surface by mist jet impingement," *Appl. Therm. Eng.*, vol. 151, pp. 459–474, 2019.
[151] C. Liang, Y. Rao, J. Luo, and X. Luo, "Experimental and numerical study of turbulent flow and heat transfer in a wedge-shaped channel with guiding pin fins for turbine blade trailing edge cooling," *Int. J. Heat Mass Transf.*, vol. 178, p. 121590, 2021.